Inelastic and deep inelastic neutron spectroscopy of water under ultra-confinement*

A.I. Kolesnikov, D.J. Wesolowski,
L.M. Anovitz – Oak Ridge National Laboratory, TN, USA

G.F. Reiter – Un. Houston, TX, USA

T. Prisk – NIST, MD, USA

A.G. Seel – University of Oxford, UK

M. Krzystyniak, G. Romanelli – ISIS, RAL, UK

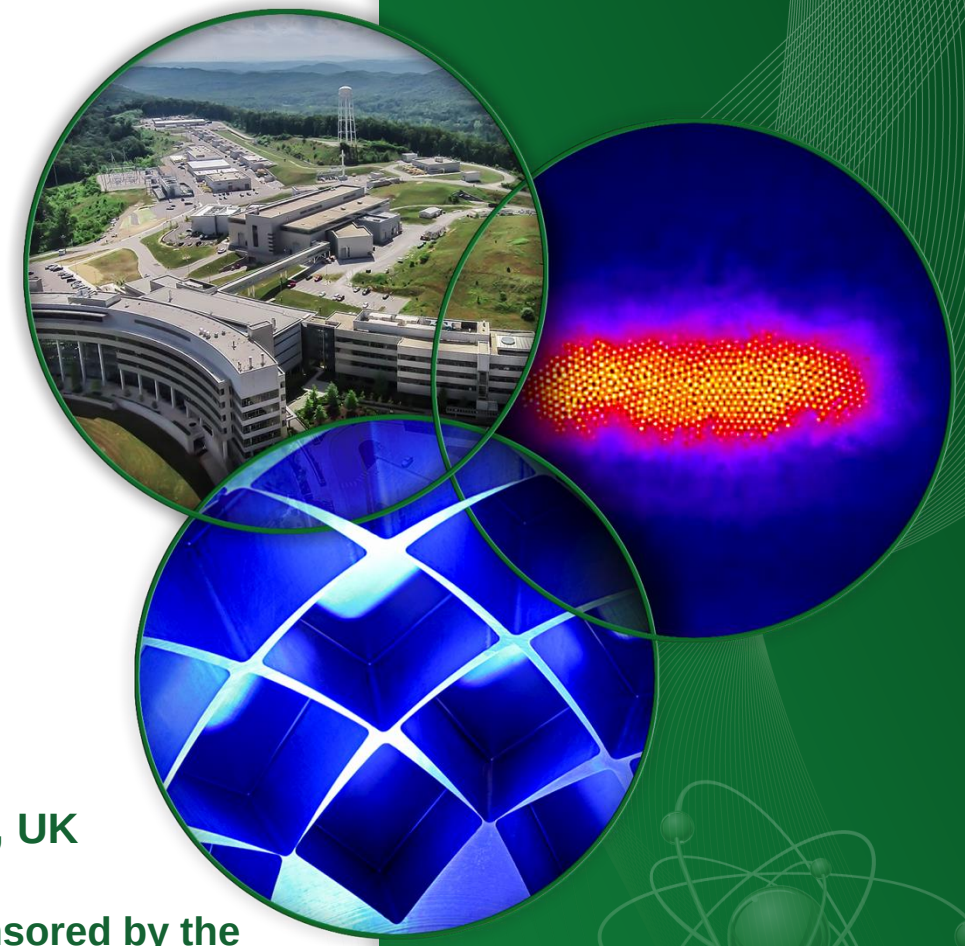

*The neutron experiment at ORNL was sponsored by the Sci. User Facilities Div., BES, U.S. DOE. This research was sponsored by the Div. Chemical Sci., Geosciences, and Biosciences, BES, U.S. DOE. The STFC RAL is thanked for access to ISIS neutron facilities.

The 85th anniversary of the discovery of the neutron by James Chadwick

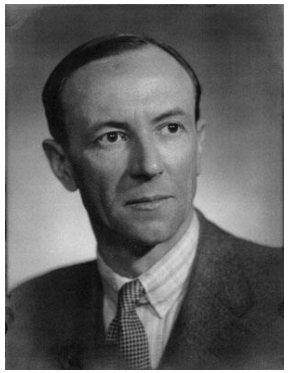

The 80th anniversary of the patent issued by the Ministero delle Corporazioni to Enrico Fermi for the use of neutrons to enhance artificial radioactivity

The 85th anniversary of the discovery of the neutron by James Chadwick

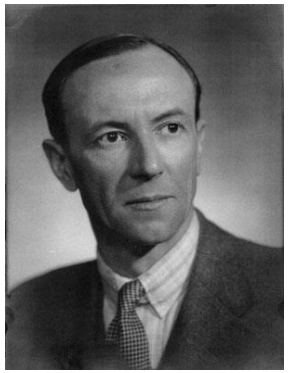

The 80th anniversary of the patent issued by the Ministero delle Corporazioni to Enrico Fermi for the use of neutrons to enhance artificial radioactivity

November 7th this year marks the 150th birthday of Marie Curie, who is one of the most famous physical chemists of all time, and was awarded two Nobel Prizes for her work in radioactivity

SNS, ORNL

Graphite Reactor

HFIR, ORNL

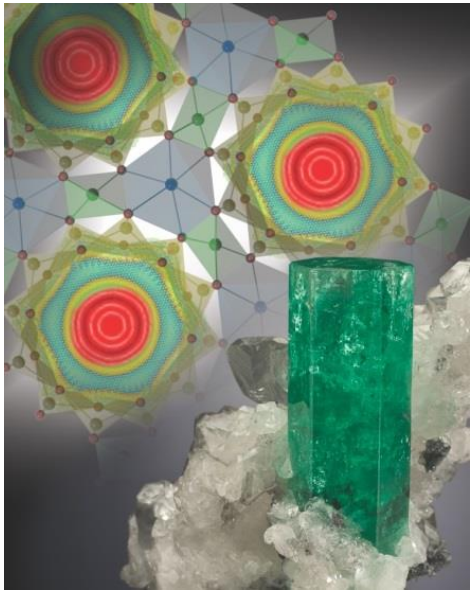

OUTLINE

- **Introduction**
- **INS study of water in beryl, Water tunneling**
- **DINS study of beryl**
- **Dynamics of water in carbon nanotubes**
- **Summary**

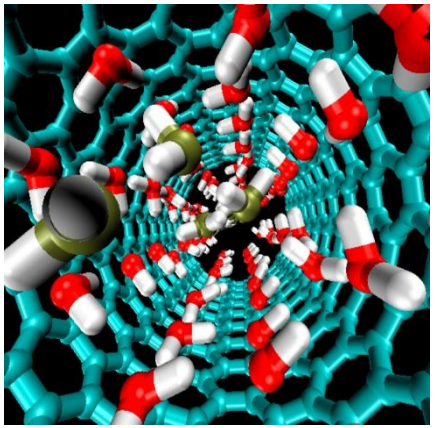

Examples of different bulk and confined water

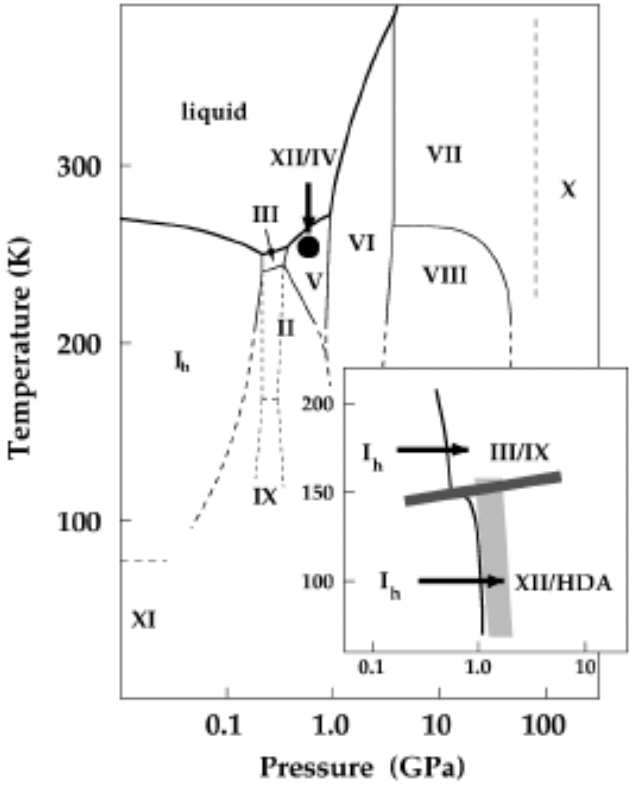

The phase diagram of ice

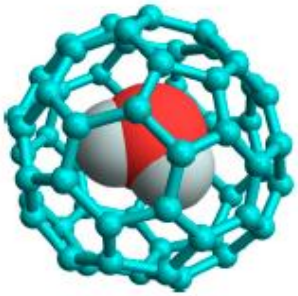

H_2O water in fullerene C_{60}

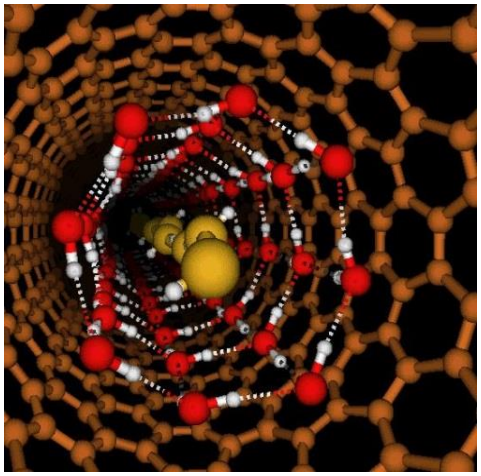

Water in SWNT

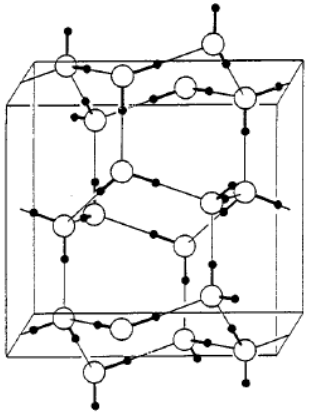

Ice-Ih

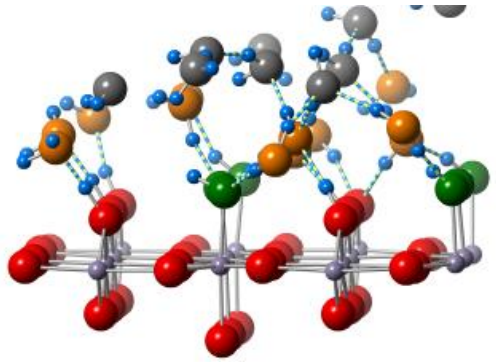

Water on surface of cassiterite (SnO_2)

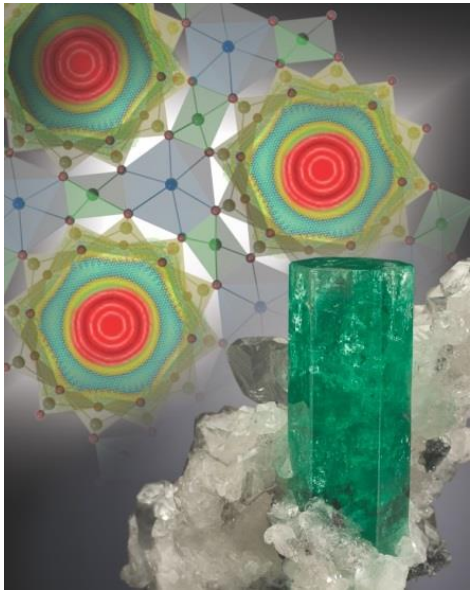

OUTLINE

- **Introduction**
- **INS study of water in beryl, Water tunneling**
- **DINS study of beryl**
- **Dynamics of water in carbon nanotubes**
- **Summary**

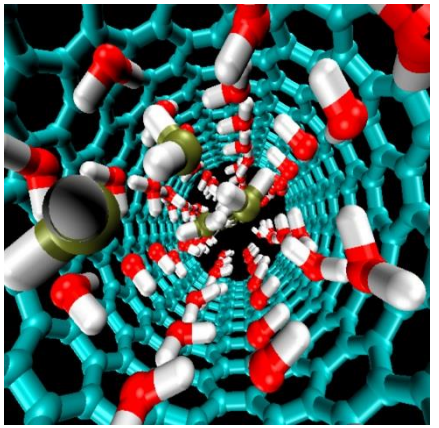

Beryl

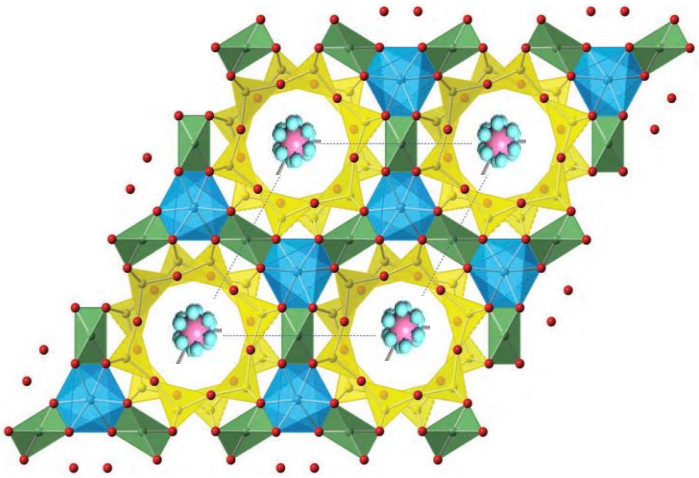

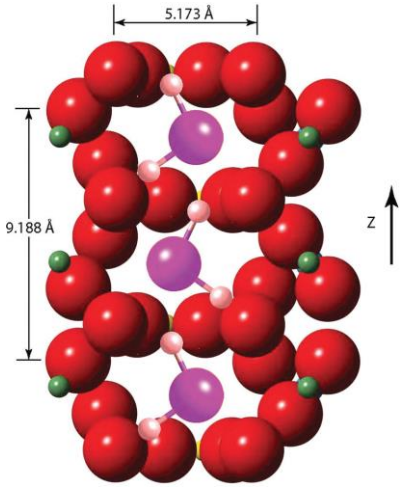

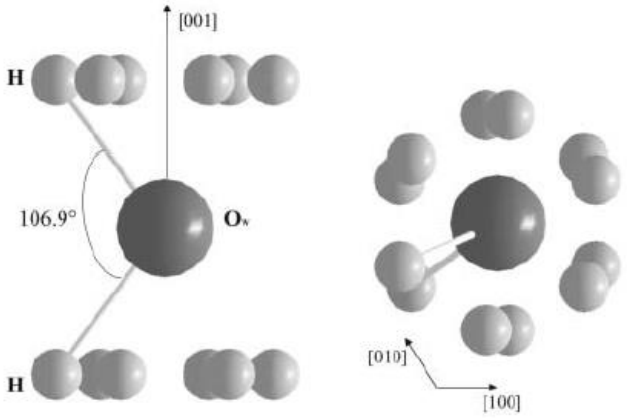

(Left) Structure of beryl ($Be_3Al_2Si_6O_{18}$•0.6H_2O, space group *P6/mcc*) showing channels running parallel to the crystallographic *c*-axis (out of the figure's plane): Si, yellow; Al, blue; O, red; and Be, green.

(Middle) Graphical representation of the alignment of water molecules inside the channels, beryl oxygen, red; water oxygen, dark pink; water hydrogen, light pink; beryllium, green; and silicon, yellow.

Topological configuration of water molecules into the channel of the alkali-poor beryl, viewed down [100] (left) and down [001] (right).

G.D. Gatta *et al*. Am. Mineral. 91 (2006) 29

CNCS: Cold Neutron Chopper Spectrometer

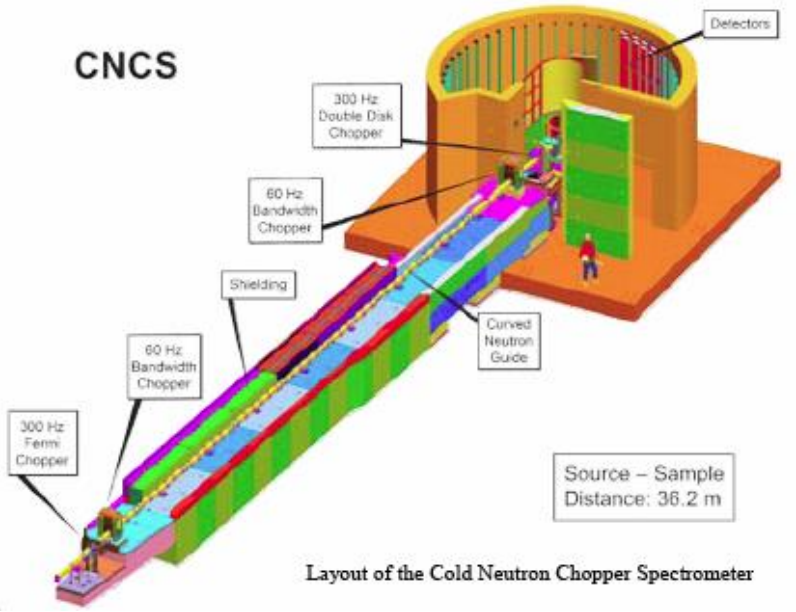

Layout of the Cold Neutron Chopper Spectrometer

E_i = <40 meV
Scattering angles:
-50 to 140° (h), ±16° (v)

SEQUOIA: The Fine Resolution Fermi Chopper Spectrometer

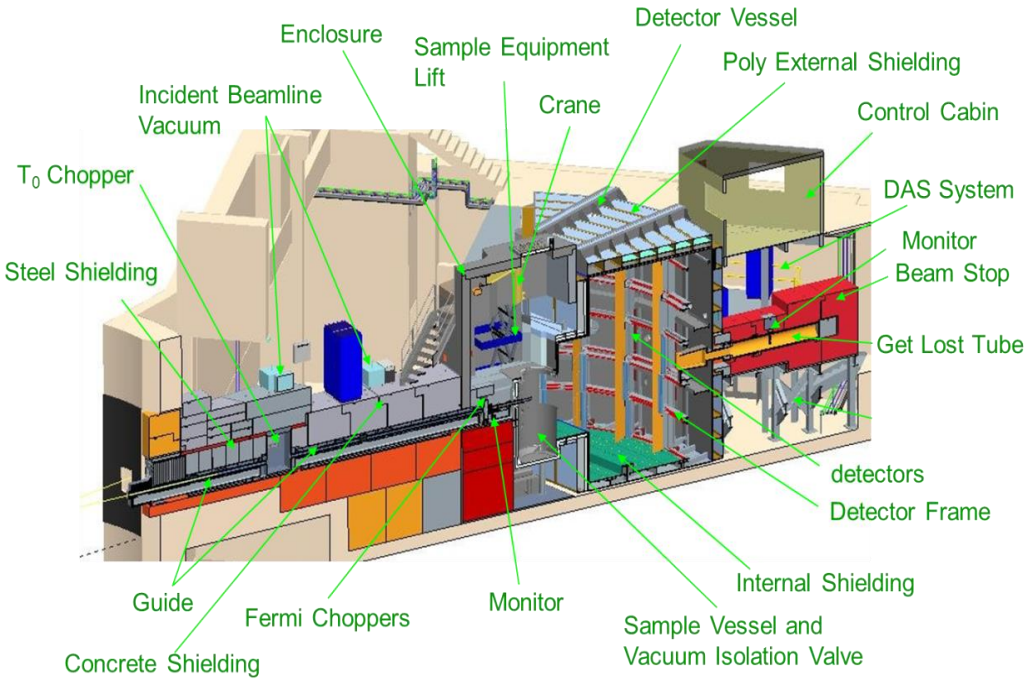

E_i = 4 − 6000 meV
Scattering angles:
-30 to 60º (h), ±18º (v)

S(Q,E) spectra of beryl, SEQUOIA

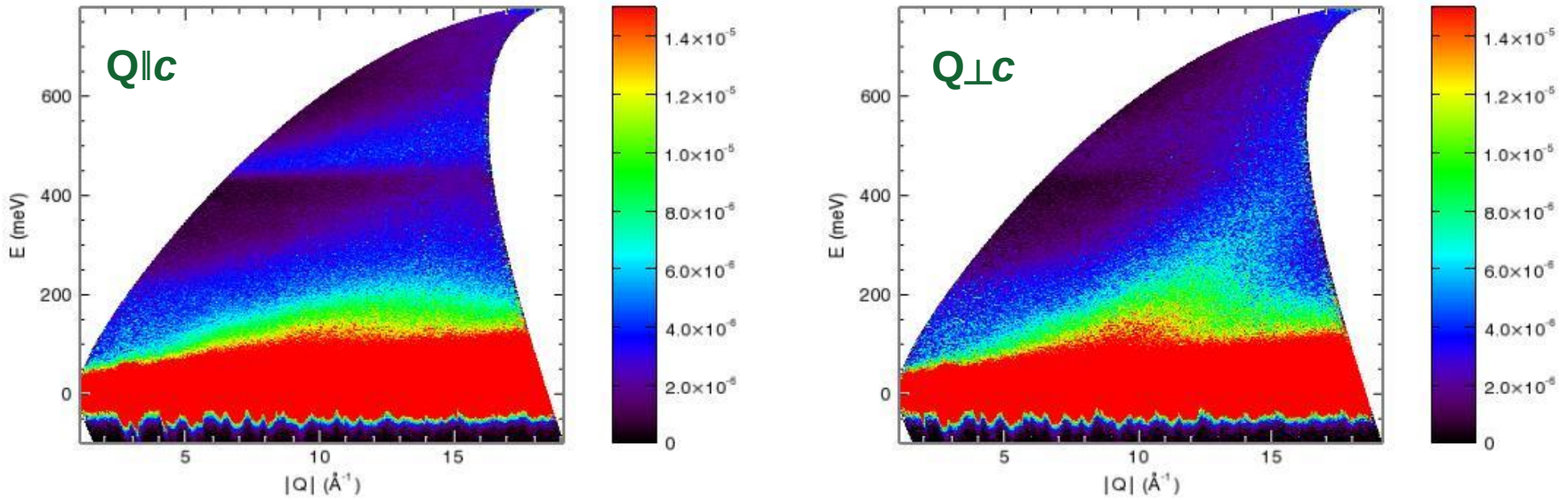

(Q,E) contour plots of S(Q,E) spectra for the neutron momentum transfer Q being perpendicular and parallel to crystallographic *c*-axis. The INS data were collected at T=6 K with E_i=800 meV.

$$S_{1ph}^{inc}(\mathbf{Q},E)=\sum_i \frac{\sigma_i \hbar^2}{6NEM_i}\exp[-(\mathbf{Qu}_i)^2][n_B(E,T)+1]\sum_{j,\mathbf{q}}\left|\mathbf{Qe}_i(j,\mathbf{q})\right|^2,$$

$$(\mathbf{Qu}_i)^2=\int\sum_{j,\mathbf{q}}\frac{\hbar^2}{6NEM_i}\,|\,\mathbf{Qe}_i(j,\mathbf{q})\,|^2[2n_B(E,T)+1]\delta[E-E(j,\mathbf{q})]dE$$

L.M. Anovitz *et al.*, Phys. Rev. E 88 (2013) 052306
A.I. Kolesnikov *et al.*, J. Phys. Chem. B 118 (2014) 13414

Beryl

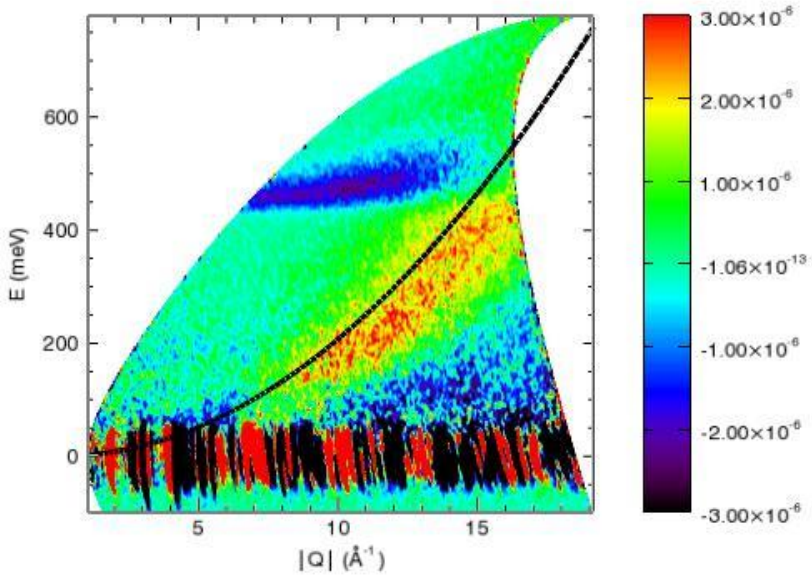

Difference between the S(Q,E) spectra from beryl at 6 K for Q⊥*c* and Q||c orientations. The solid line shows the neutron recoil spectrum for free particle of mass *m*=1 a.u., $E=\hbar^2Q^2/2m$.

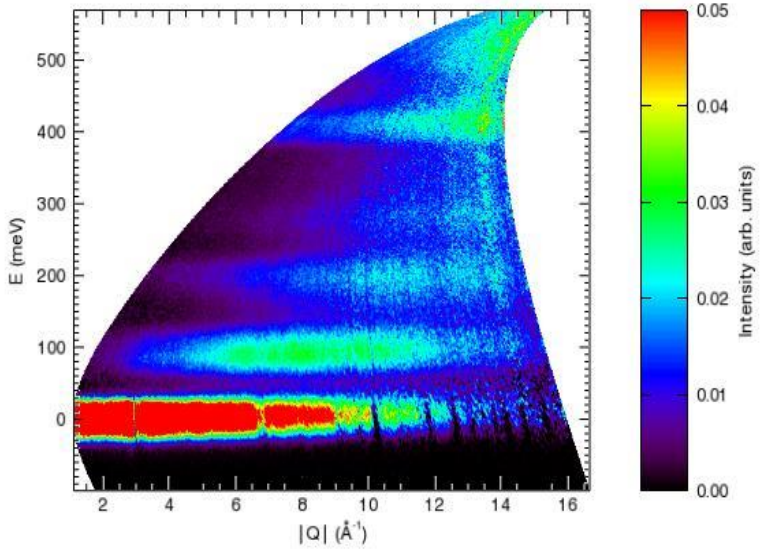

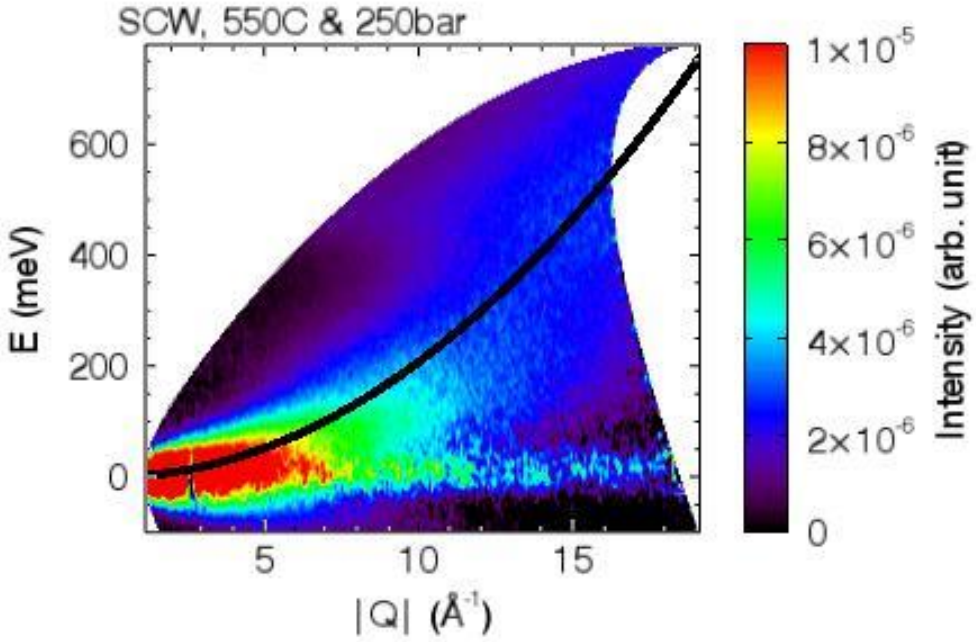

INS spectra of ice-Ih at T=6 K (left) and supercritical water at T=280 K and P=250 bar (top, right).

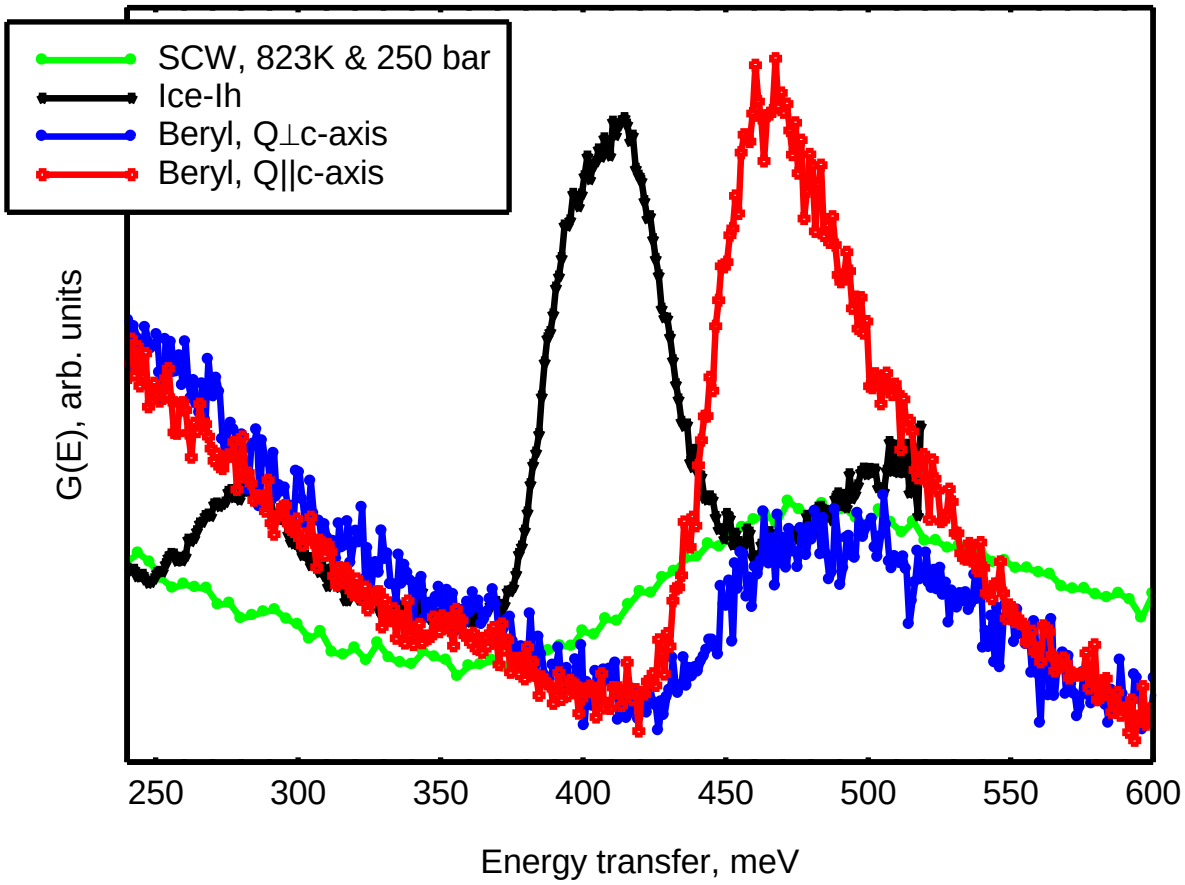

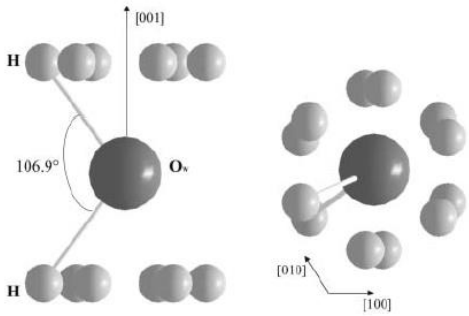

INS spectra at T=6 K for beryl measured with neutron momentum transfer Q parallel and perpendicular to the crystallographic *c*-axis; E_i=800 meV, compared to supercritical water at T=823 K & P=250 bar, and ice-Ih at T=6 K (E_i=600 meV). The confined water intramolecular O-H stretching peak is at 465 meV.

Beryl

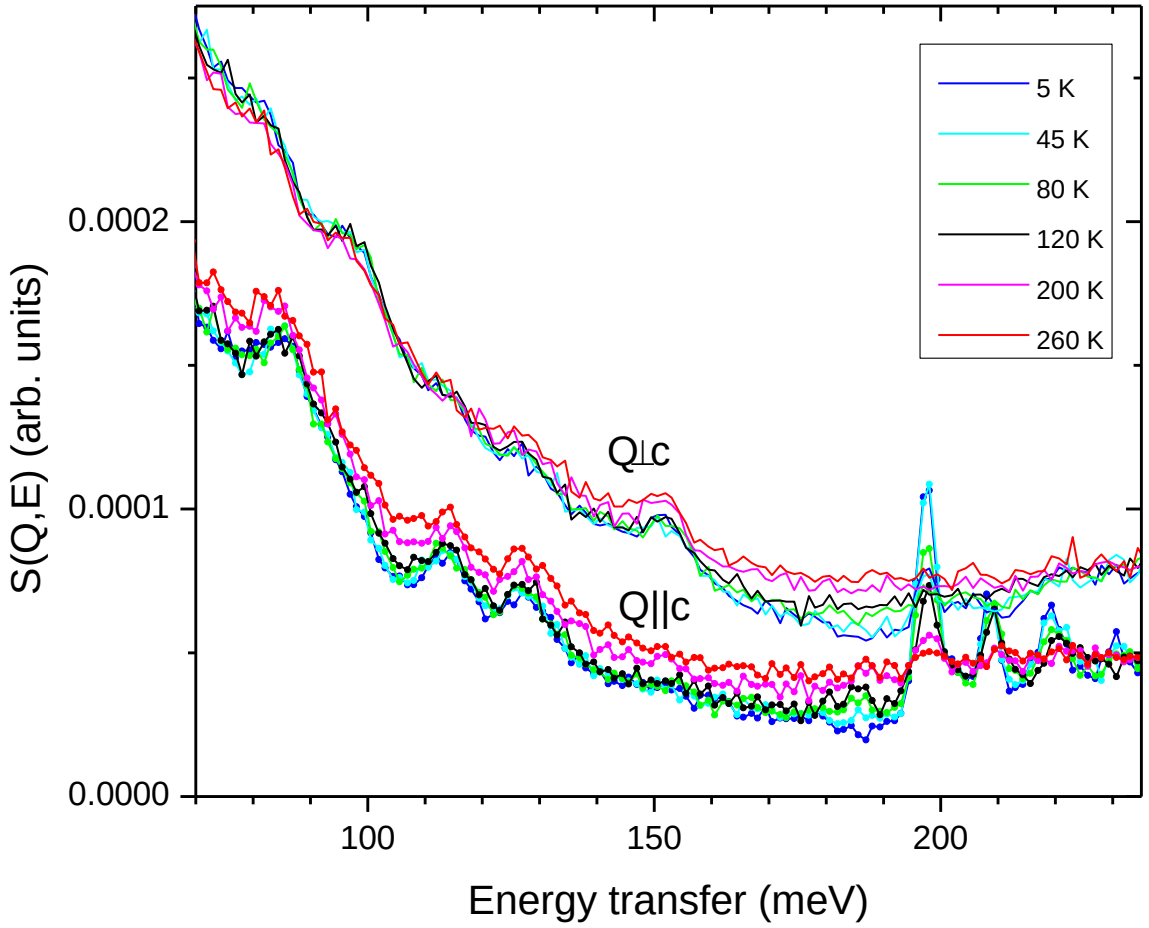

INS spectra for E_i=250 meV. The peak at 197 meV is due to H-O-H bending mode (ν_2), E_{bend}=197.3+0.26(459.7-E_{str}), [1]. Three peaks at the right are due to multi-phonon neutron scattering involving ν_2 and translational modes (~11 meV) of water molecule along the *c*-axis.

[1] M. Falk, Spectrochim. Acta A40 (1984) 43.

Beryl

Q∥*c*

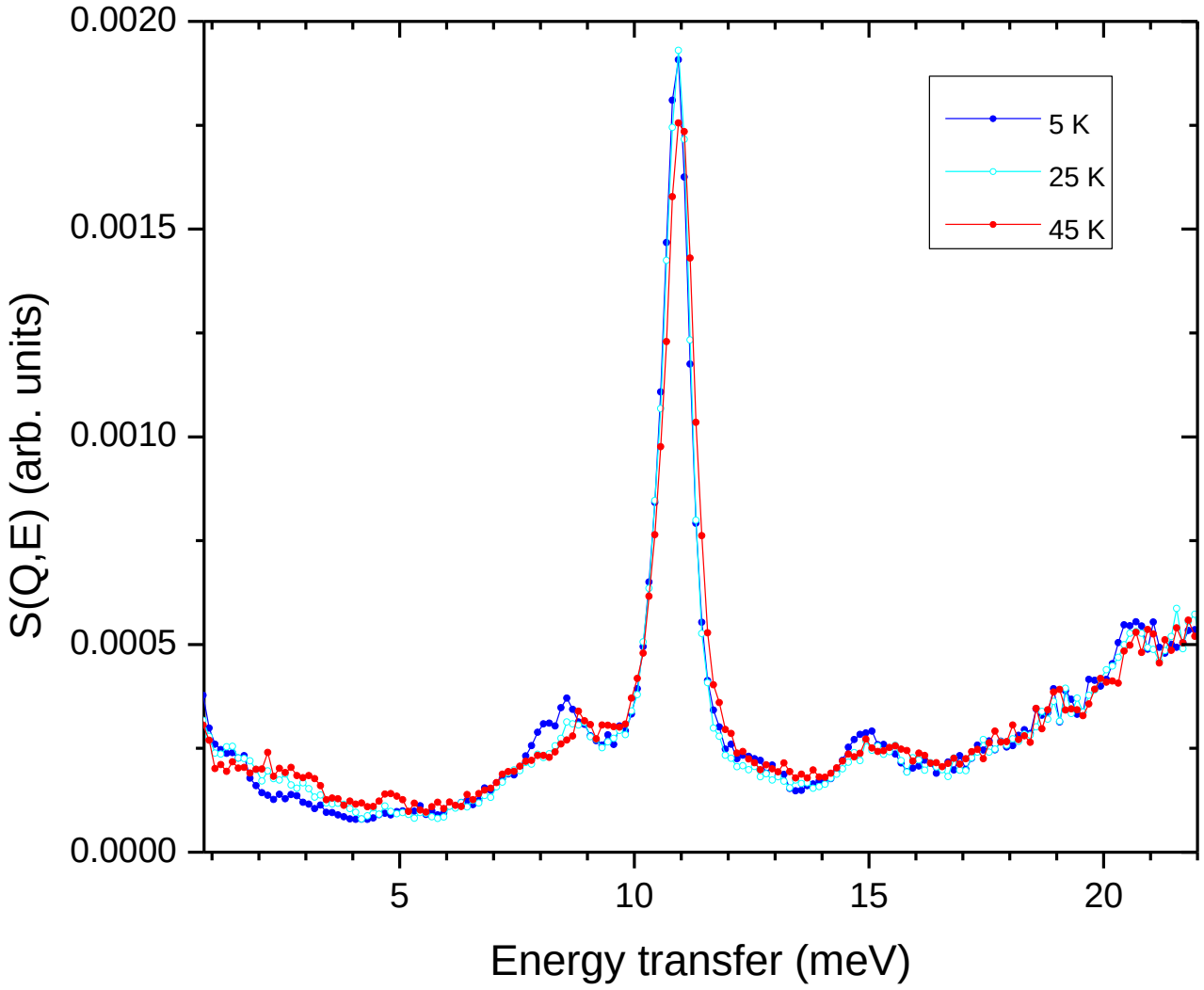

INS spectra of water in beryl, E_i=25 meV, Q parallel to the *c*-axis.

Beryl

$Q \perp c$

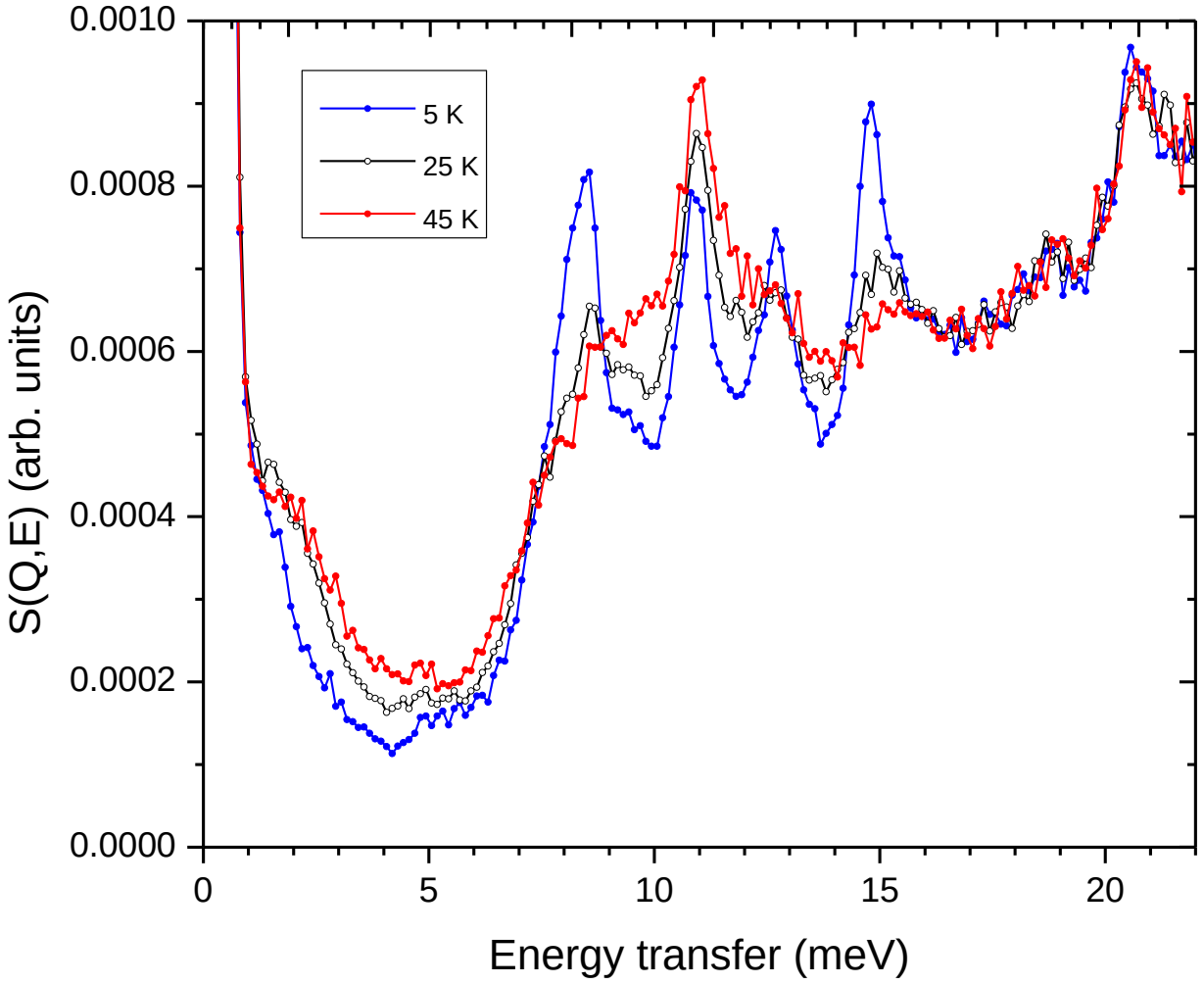

INS spectra of beryl, E_i=25 meV, Q perpendicular to the *c*-axis. The intensity of the peaks at 8.4, 12.7 and 14.7 meV strongly decrease with temperature increase.

Beryl

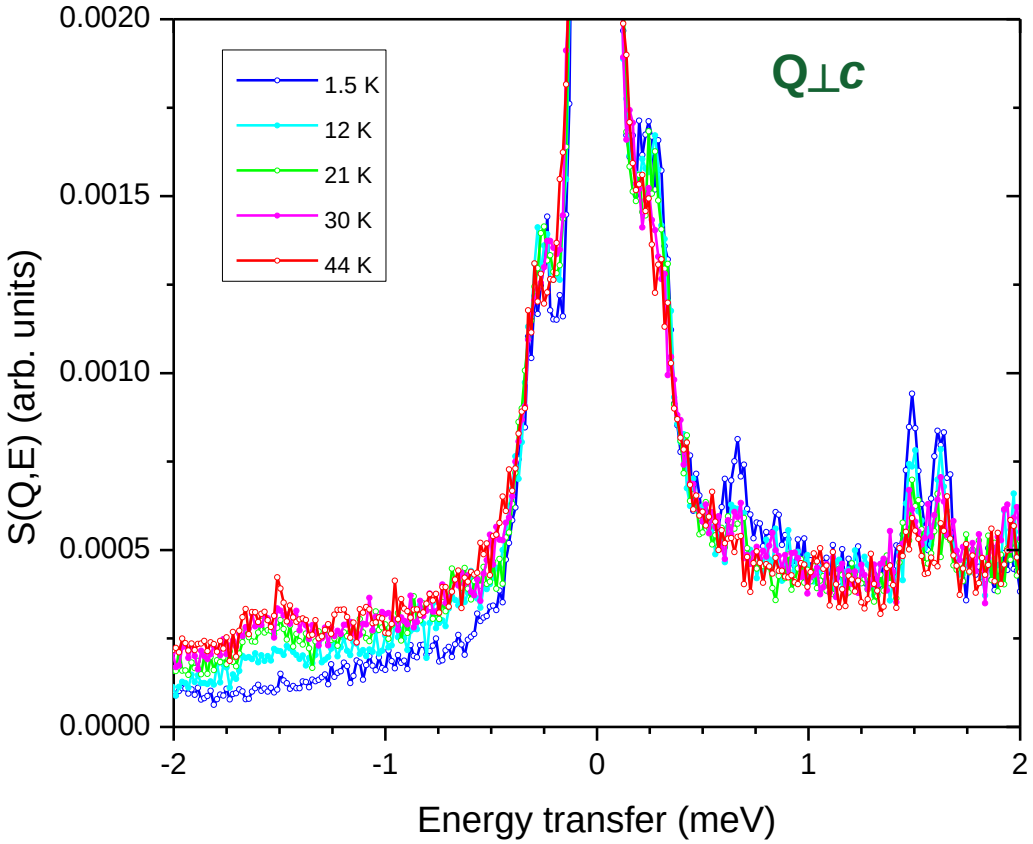

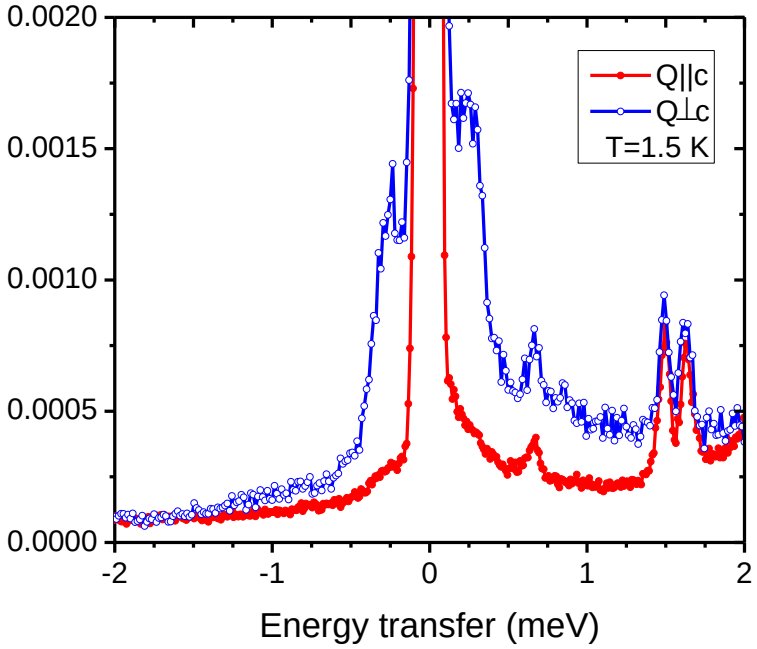

INS spectra of beryl at different temperatures measured with E_i=3 meV at CNCS, Q perpendicular to the *c*-axis (left figure). The intensity of the peaks at 0.27, 0.66, 1.49 and 1.63 meV in energy loss site strongly decrease with temperature increase. The peaks at 0.66, 1.49 and 1.63 meV are isotropic (right figure)

Beryl

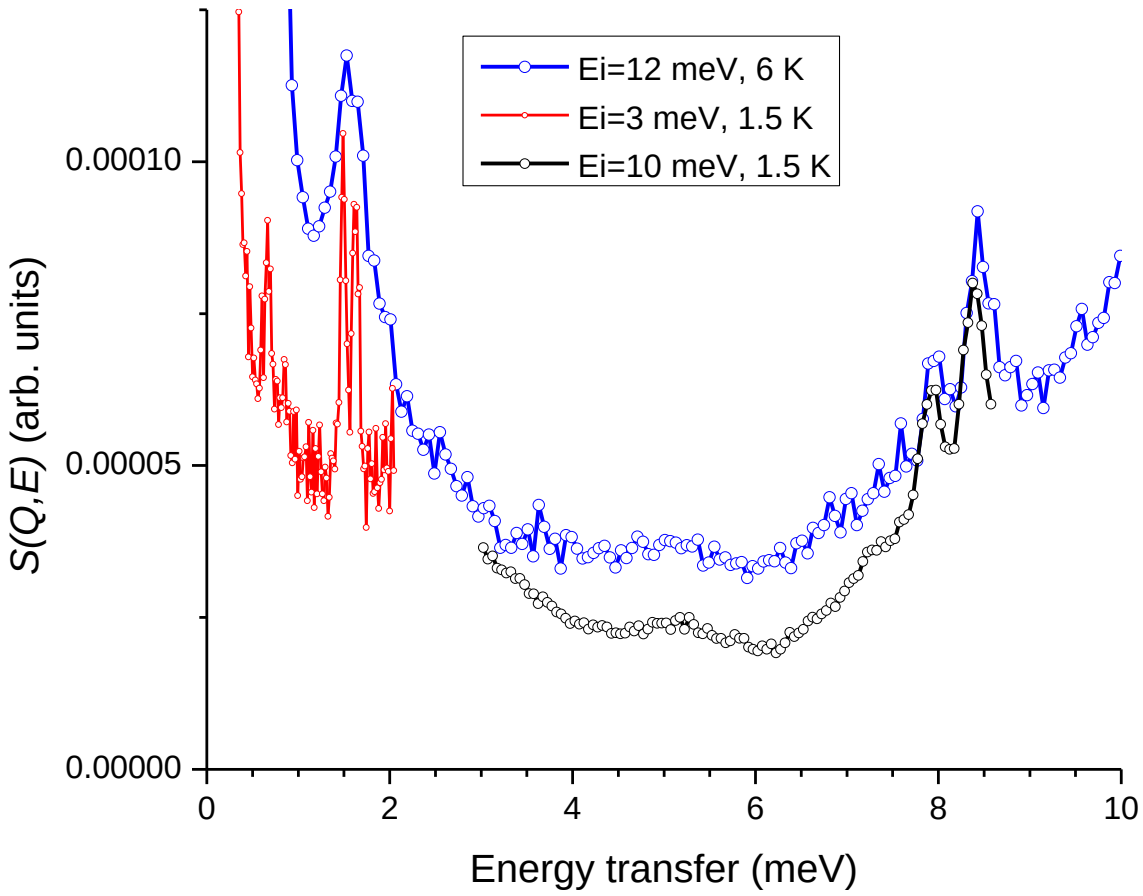

INS spectra of beryl for Q perpendicular to *c*-axis measured at SEQUOIA with E_i=12 meV, and at CNCS with E_i=10 meV, showed that the peak at 8.4 meV is split (7.9 and 8.4 meV).

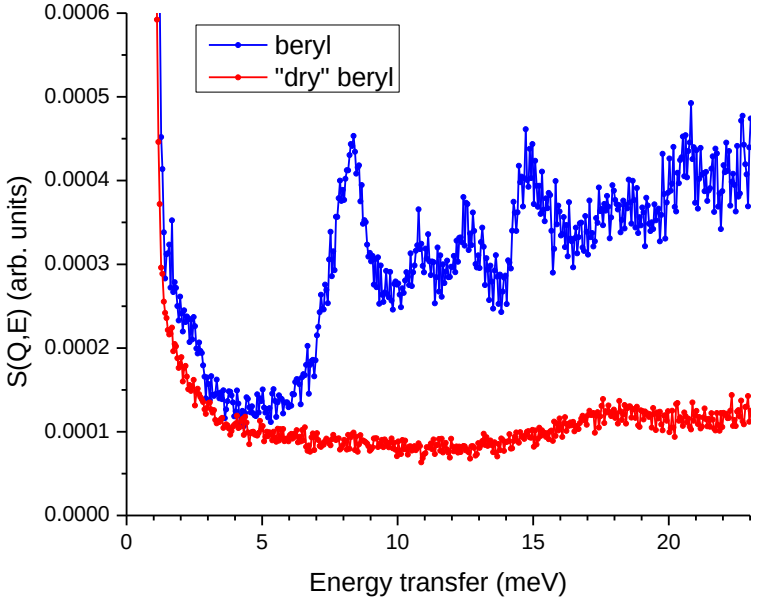

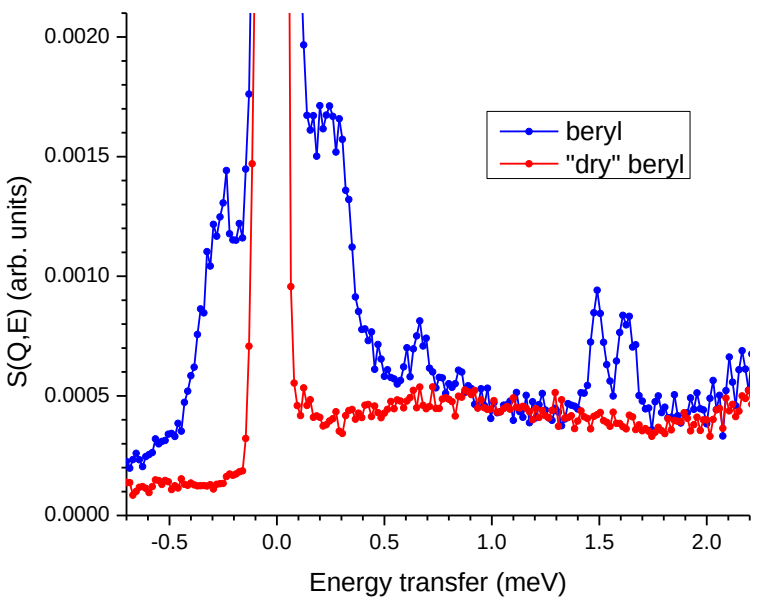

INS spectra of beryl and dehydrated ("dry") beryl measured *at T*=1.5 K with Q⊥*c*-axis using CNCS spectrometer with E_i=28 and 3 meV (left and right, respectively). The spectra of the "dry" beryl show small intensity (due to smaller neutron scattering cross-sections of atoms in beryl compared to hydrogen) with very smooth featureless behavior, probably due to overlapping of many possible modes in this energy range.

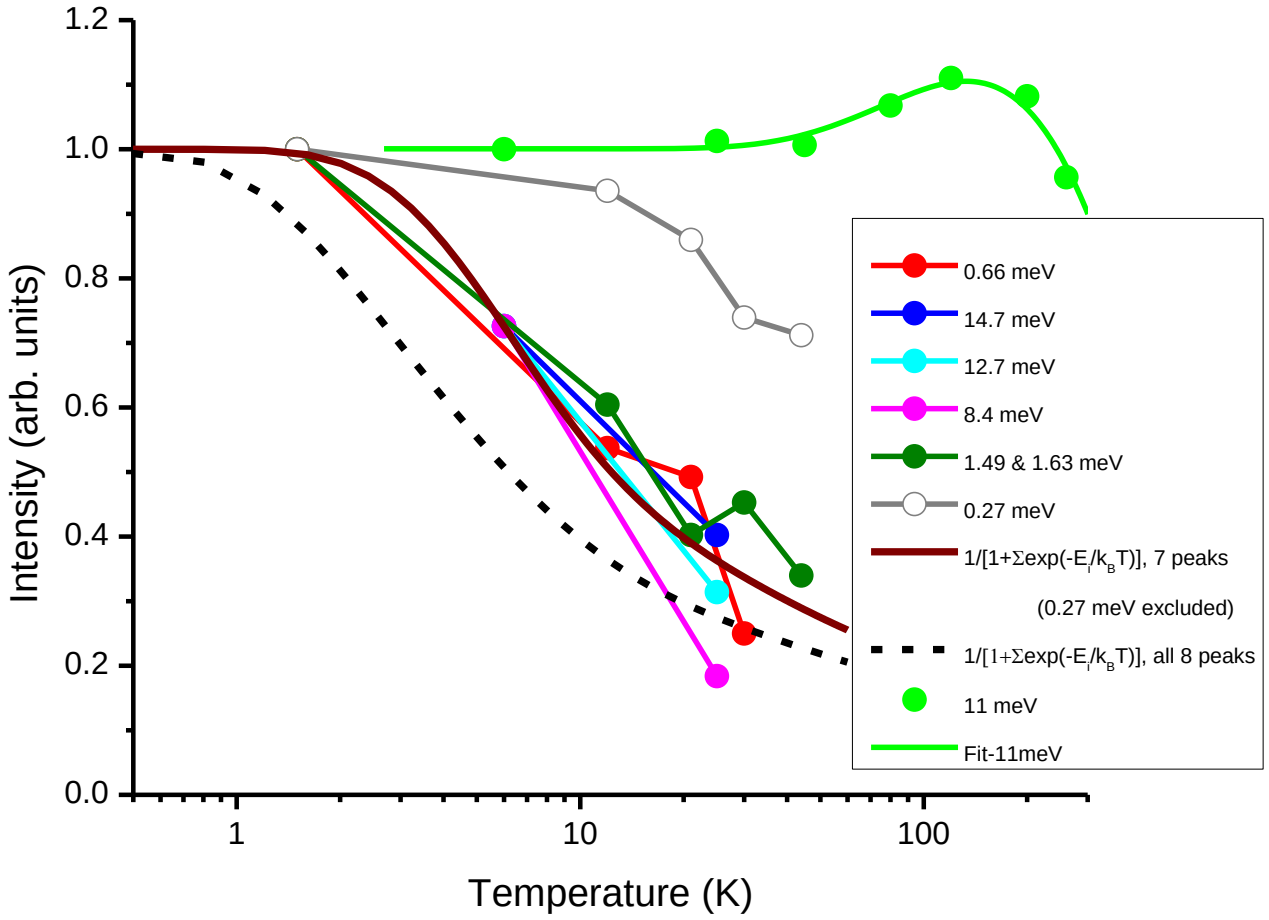

The reduced intensities of the tunneling peaks at energies E_i=0.27, 0.66, 1.49 & 1.63, 7.9 & 8.4, 12.7 and 14.7 meV for Q⊥*c*-axis of beryl (except for the peak at 0.27 meV) follow the temperature dependence for transitions from the lower to higher split ground states, $\mathrm{I(T)} \propto 1/\left\{1+\sum_{i=1}^{7} exp(-\frac{E_i}{k_B T})\right\}$. The intensity of the translational (vibrational) mode at 11 meV (Q||*c*-axis) is shown for comparison. The peaks' intensities are normalized to be 1 at T=0 K.

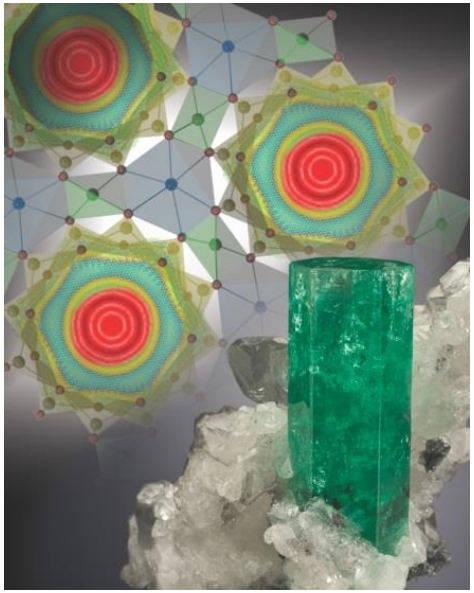

OUTLINE

- **Introduction**
- **INS study of water in beryl, Water tunneling**
- **DINS study of beryl**
- **Dynamics of water in carbon nanotubes**
- **Summary**

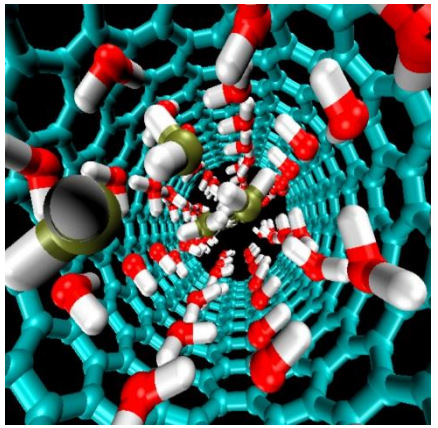

Deep Inelastic Neutron Scattering

The momentum distribution $n(\mathbf{p})$ of the particles can be measured by Deep Inelastic Neutron Scattering (DINS). DINS is inelastic neutron scattering in the limit of large momentum transfer, Q (~30-100 Å^{-1}). $S(\mathbf{Q}, E)$ in this limit takes the form:

$$S(\mathbf{Q}, E) = \int n(\mathbf{p}) \delta \left(E - \frac{\hbar^2 \mathbf{Q}^2}{2M} - \frac{\hbar \mathbf{Q} \mathbf{p}}{M} \right) d\mathbf{p}$$

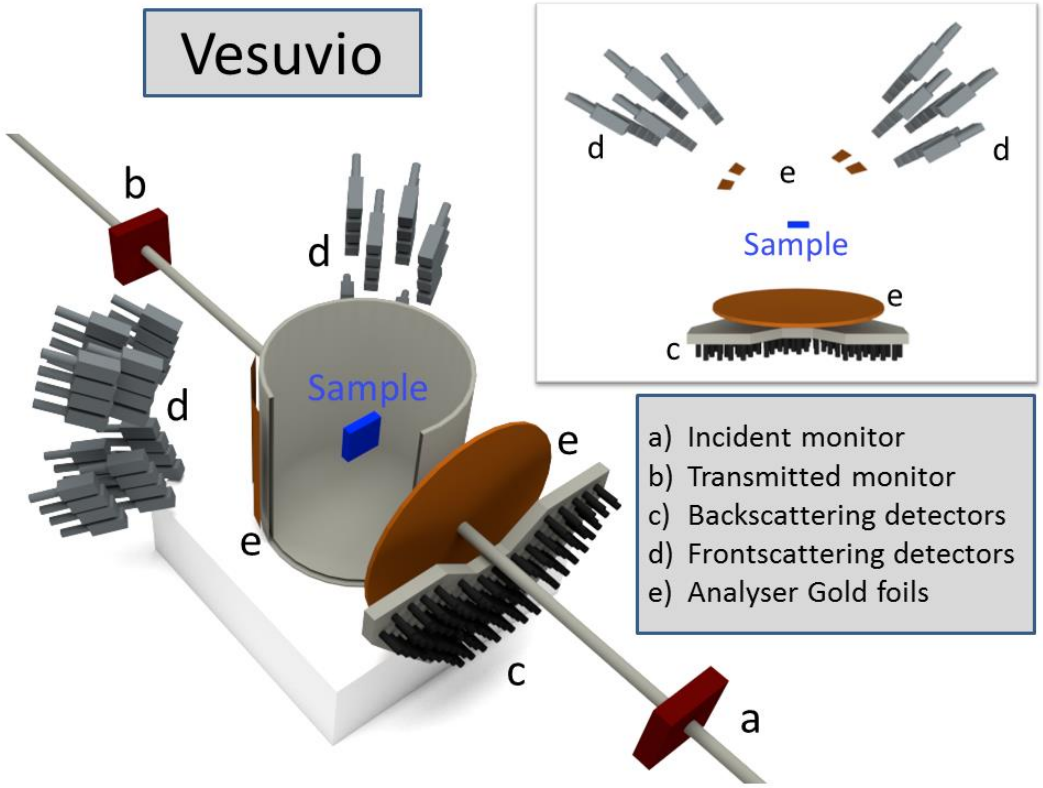

Analyzing energy: 4906 meV (Au)

DINS measurements were done at 4.3 K for two crystal orientations, with *c*-axis along and perpendicular (*c*-axis vertical) to the incoming neutrons. The spectra were transferred to the 3D momentum distribution of water protons in beryl *n(p)* by simultaneous fit of all data using the Hermite polynomials of the 8 order (George Reiter, Un. Houston, TX).

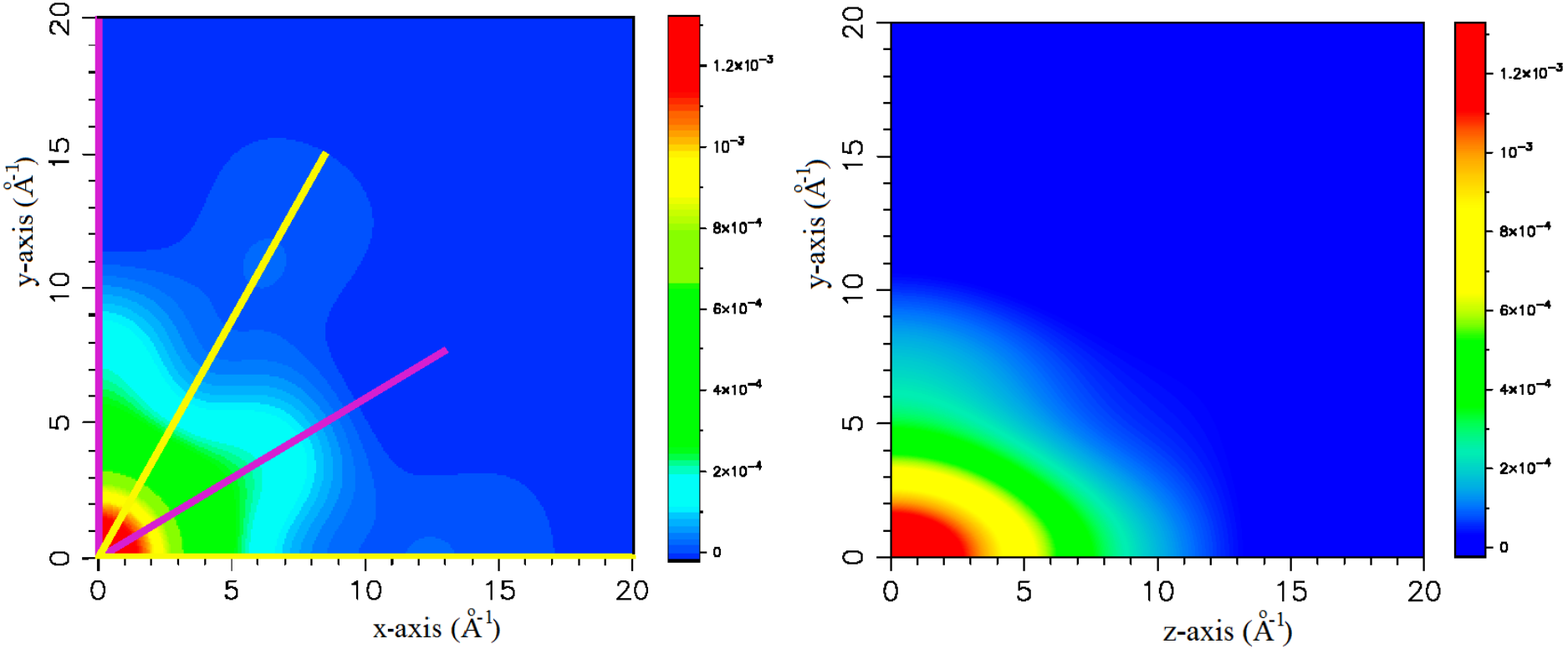

Projection of water proton momentum distribution *n*(p) onto the *xy*- and *yz*-planes.

The values of *n(p)* broadening are: σ_x=3.66, σ_y=3.61 and σ_z=4.98 Å^{-1}, therefore the kinetic energy of the proton, $\langle E_K \rangle = \frac{\hbar^2}{2M}\left(\sigma_x^2 + \sigma_y^2 + \sigma_z^2\right)$=106 meV, is much smaller than has been observed in bulk water (~150 meV).

The water proton kinetic energy can be estimated by using semi-empirical approach in quasi-harmonic approximation (Moreh and Nemirovsky, *J. Chem. Phys.* 133 (2010) 084506)

$$E_K = S_t \int_0^{v_t} \alpha_t g_t(v) dv + S_r \int_{v_{r1}}^{v_{r2}} \alpha_r g_r(v) dv + \sum_{j=1}^{3} S_j \frac{1}{2} \left(\frac{h v_j}{e^{h v_j / kT} - 1} + \frac{h v_j}{2} \right)$$

$$\alpha_i = \left(\frac{h v_i}{e^{h v_i / kT} - 1} + \frac{h v_i}{2} \right)$$

and S_j is the kinetic energy fraction of atom *j*, which for water proton is about 0.47.

In the case of beryl, using only the intramolecular vibrations of water obtained from INS spectra ($v_1 = v_3 = 465$ meV, and $v_2 = 197.5$ meV) and omitting the translational and librational vibrations of water the estimated

$$E_K = 0.47 \times (2 \times 465/2 + 197.5/2)/2 = 133 \text{ meV},$$

which is larger, than the observed (DINS) experimental value, E_K=106 meV.

Quantum behavior of water nano-confined in beryl

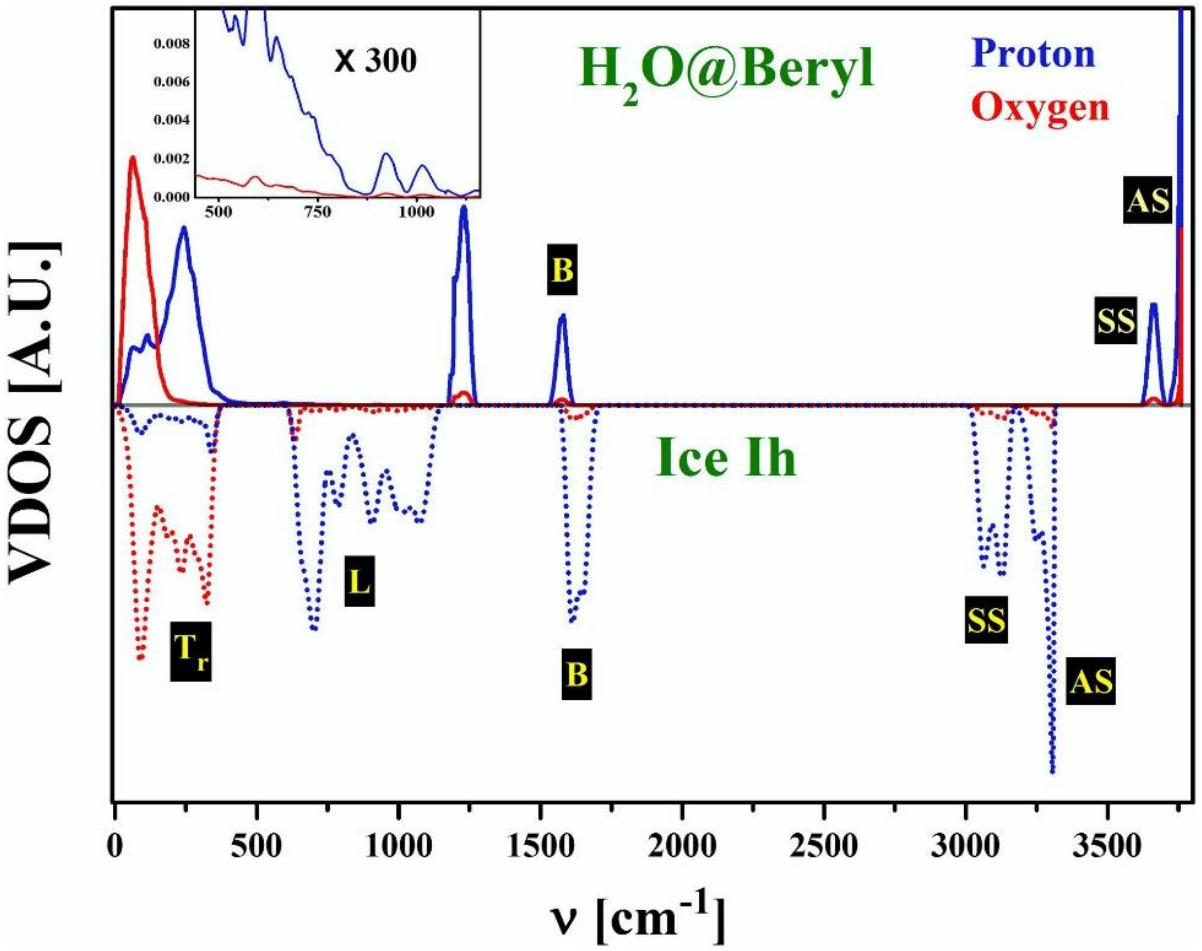

The water proton E_K in beryl at 5 K was obtained by simulating the partial VDOS from DFT calculations. The result, E_K=104.4 meV, is in remarkable agreement with the DINS measured value of 106 meV. The calculation indicates that the vibrational states of the proton of the nano-confined water molecule distribute much differently than in ordinary H_2O phases, most probably due to coupling with lattice modes of the hosting beryl nano-cage.

Y. Finkelstein *et al*., J. Chem. Phys. 146 (2017) 124307

TABLE VI (Y. Finkelstein *et al*., J. Chem. Phys. 146 (2017) 124307). DFT calculated kinetic energy fractions (F) shared by the H and O atoms in pure ice Ih and in H_2O@Beryl at 5 K. Tr, L, B, SS, and AS correspond to translation, libration, bending, symmetric and asymmetric stretch, respectively. Note that while the two low energy bands in the nano-confined H2O are labeled by N/A (not assigned) due to their uncertain assignments, the high energy bands purely arise from the internal vibrations of H2O. The last row depicts the DFT calculated E_K and the DINS values at 5 K (in meV units).

	DFT							DINS	
	Ice				H_2O @Beryl			Ice	H_2O@Beryl
Mode	H	O	Σi	Mode	H	O	Σi	H	
T_r	0.0553	0.8878	0.9984	N/A	0.5519	0.9418	2.0456		
L	0.4744	0.0535	1.0023	N/A	0.2068	0.0270	0.4406		
B	0.4700	0.0625	1.0113	B	0.2151	0.0315	0.4617		
SS	0.4734	0.0554	1.0022	SS	0.2427	0.0279	0.5133		
AS	0.4677	0.0582	0.9936	AS	0.2661	0.0342	0.5664		
Ke(H,O)	154.6	36.2			104.4	19.2		152	105
Σj	3.0012	3.0			3.0	3.0			

$$E_K(H) = \frac{3}{2}\int_{v_0}^{v_f} g_H(v)\alpha(v,T)dv \,/\, \int_{v_0}^{v_f} g_H(v)dv, \qquad \alpha(v,T) = \left(\frac{hv}{e^{hv/kT}-1} + \frac{hv}{2}\right)$$

The phonons eigenvectors $\mathbf{e}(i|\mathbf{k}j)$ should satisfy two sum rules, "the orthonormality and closure conditions" (G.K.Horton&A.A.Maradudin, Dynamical Properties of Solids, V.1, Amsterdam, 1974)

$\sum_{i=1}^{3}|\mathbf{e}(i|\mathbf{k}j)|^2 = 1$, and $\sum_{j=1}^{9}|\mathbf{e}(i|\mathbf{k}j)|^2 = 1$

Σi=2xF(H)+F(O), and Σj=3x(Tr+L)+B+SS+AS

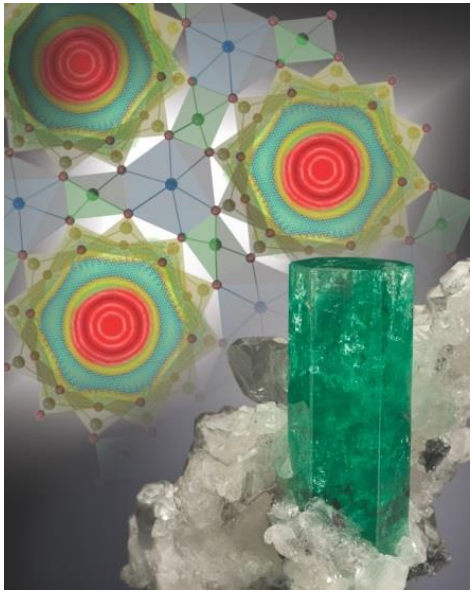

OUTLINE

- **Introduction**
- **INS study of water in beryl, Water tunneling**
- **DINS study of beryl**
- **Dynamics of water in carbon nanotubes**
- **Summary**

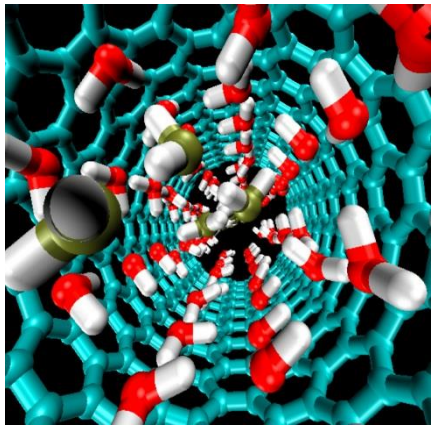

Water in SWNT

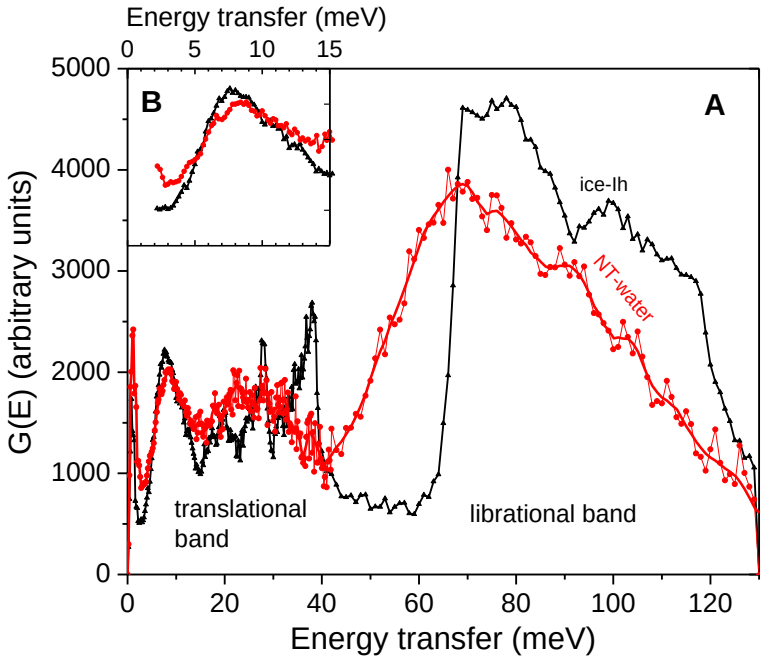

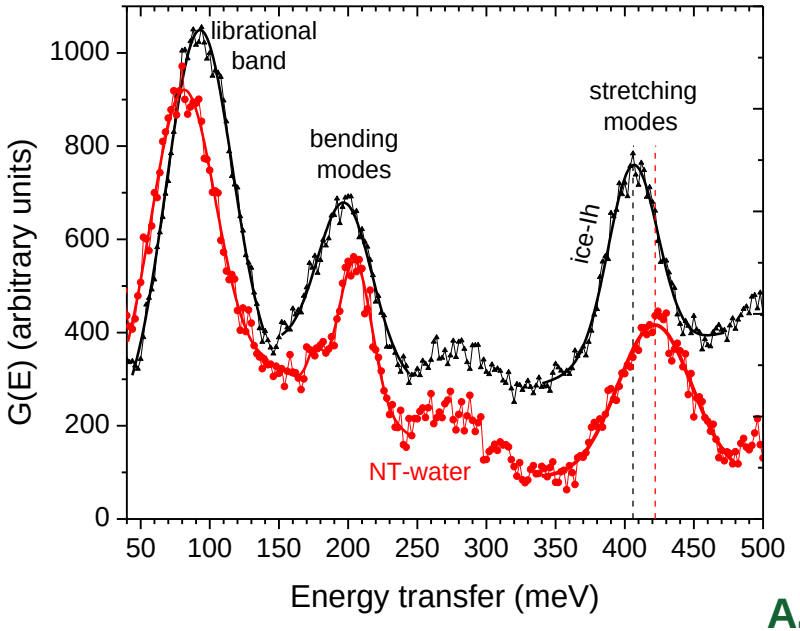

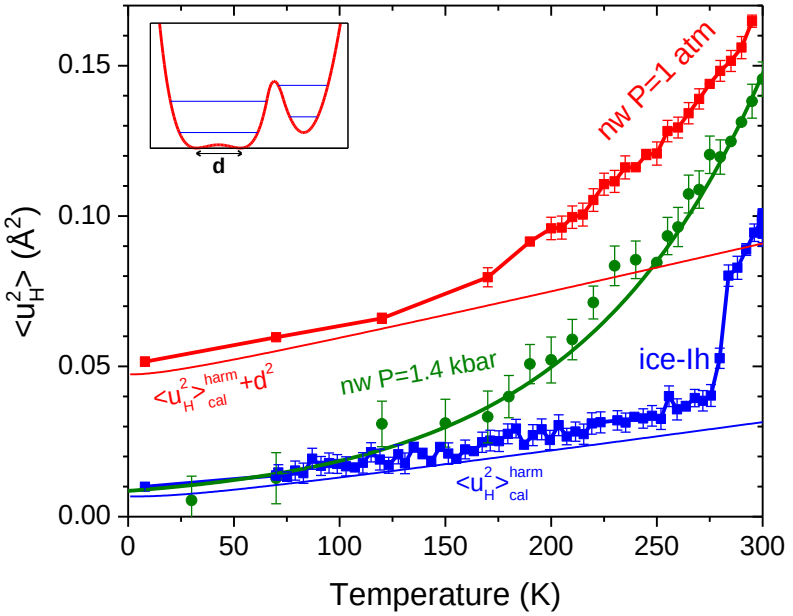

MSD of water protons in SWNT compared to ice-Ih obtained from QENS.

Vibrational spectra of water in SWNT compared to the spectrum of ice-Ih.

A.I. Kolesnikov *et al.*, Phys. Rev. Lett. 93 (2004) 035503

Water in SWNT

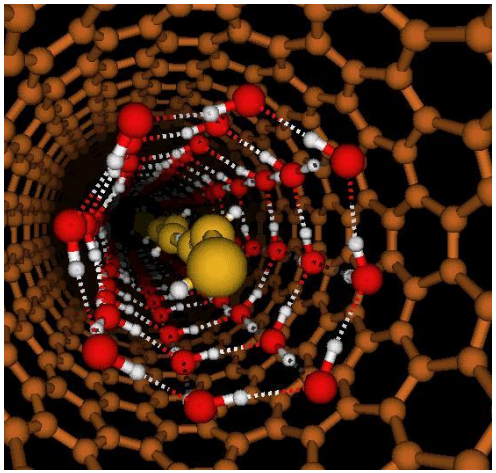

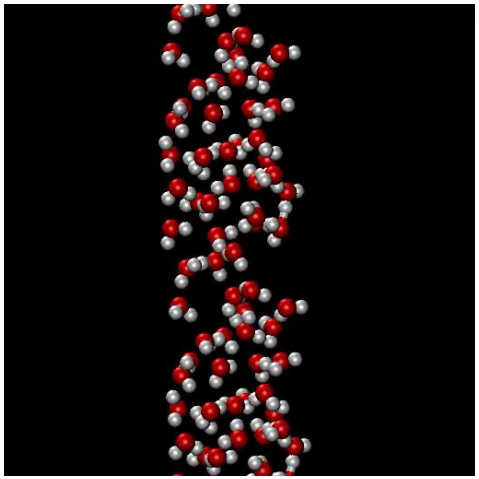

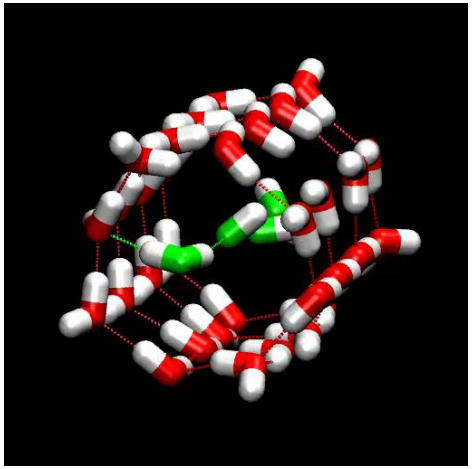

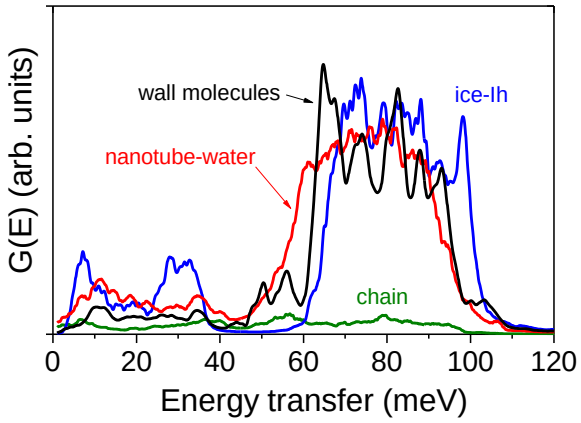

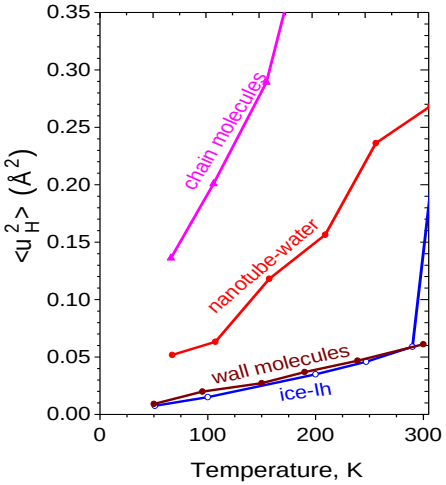

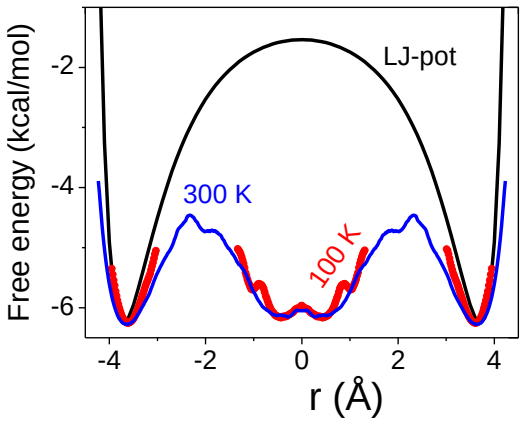

MD calculations (Christian Burnham) with TTM2-F polarizable flexible water model (uses smeared charges and dipoles) [1]. MD simulations consist of 40 Å long carbon nanotube in periodic boundary conditions that interacts with water via the LJ potential [2].

[1] Burnham & Xantheas, J. Chem. Phys. (2002); [2] Walther *et al.*, J. Phys. Chem. (2001)

Deep-Inelastic Neutron Scattering

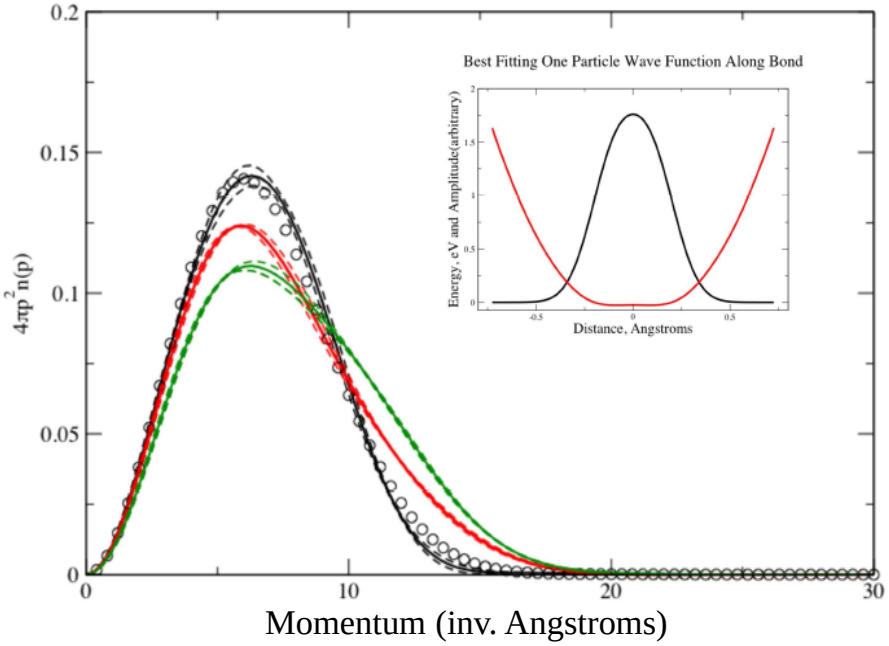

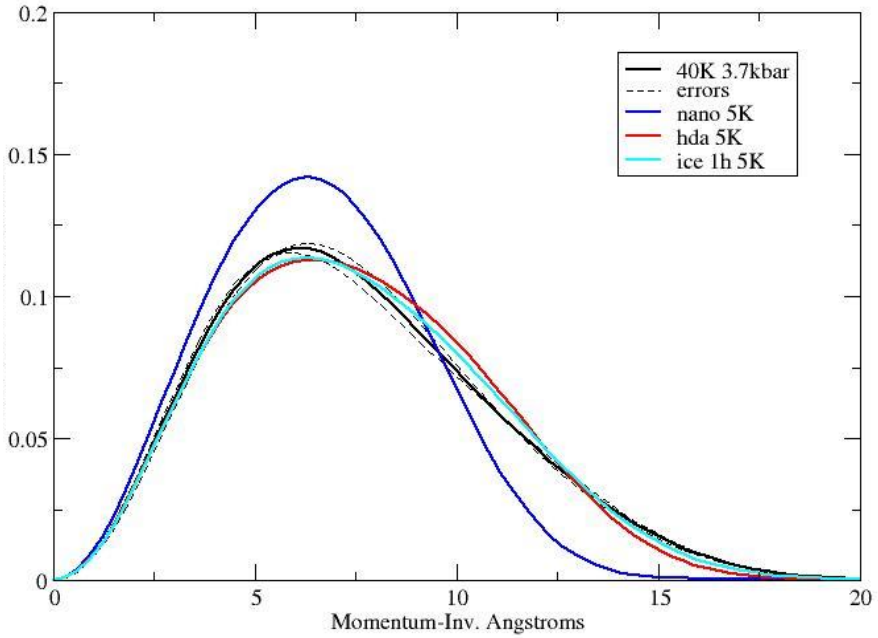

Momentum distributions for NT-water at 268 K (green) and 5 K (black), and ice-Ih at 269 K (red). The circles are a fit to a model in which the water proton is delocalized in a double well potential. The potential (red) and wave-function (black) are shown in the inset.
$\langle E_K \rangle$=104 meV for NT-water at 5 K,
$\langle E_K \rangle$=146-152 meV for bulk water.

G. Reiter *et al.*, Phys. Rev. Lett. 97 (2006) 247801

The momentum distribution of the protons in NT-water at P=1 bar (T=5 K) and P=3.7 kbar (T=40 K) compared with bulk ice-Ih and hda-ice (T=5 K) at P=1 bar.

Summary

- **INS spectra of beryl at low temperature show 8 peaks at energies 0.25–15 meV, and the intensity of these peaks strongly decreases with increasing temperature. The data can be explained by transitions between the split ground states of confined water due to its tunneling between the 6-fold equivalent positions across the crystal channels.**

- **DINS data show that water protons exhibit 6-fold momentum distribution across the beryl channel, with additional maxima due to proton coherent delocalization (tunneling). The obtained proton kinetic energy, E_K=106 meV, is much smaller than in bulk water (~150 meV), in spite of the observed highest possible O-H stretching modes.**

- **INS and QENS measurements of water in SWNT showed very soft dynamics of nanotube-water. MD simulations identified an ice-wall plus water-chain structure at low temperatures. The soft dynamics of nanotube-water arise mainly from the drastic change in hydrogen-bond connectivity of the central water-chain with an average coordination number less than 2 (compared to 4 in bulk ice).**

- **DINS showed that the quantum state of the nanotube-water protons at low temperature is qualitatively different from that of bulk water, and gave very small value for kinetic energy, E_K=104 meV.**

Acknowledgements

George Ehlers	ORNL
Eugene Mamontov	
Andrey Podlesnyak	
Narayani Choudhury	Un. Washington, Bothell, WA
Jean-Marc Zanotti	IPNS, ANL
Chun-Keung Loong	
Pappannan Thiyagarajan	
Alexander P. Moravsky	MER Corporation, Tucson, AZ
Christian J. Burnham	University of Utah, UT
J. Mayers	ISIS, RAL, UK

DFT simulations (Narayani Choudhury, Un. Washington) reveals proton delocalization in beryl, with a lateral spread of about 1.2 Å, consistent with the experiments. Lattice excitations of the beryl cage couple with local modes of water and yield adiabatic coincidence states in the vicinity of which the energy barriers for water rotation are significantly lowered, and the confined water molecules exhibit quantum tunneling.

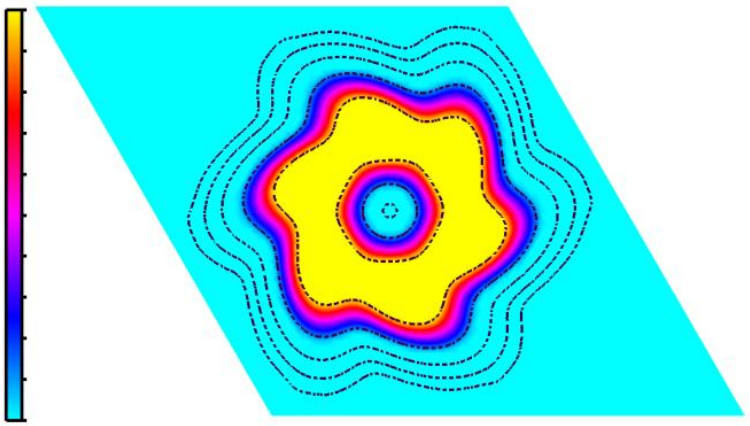

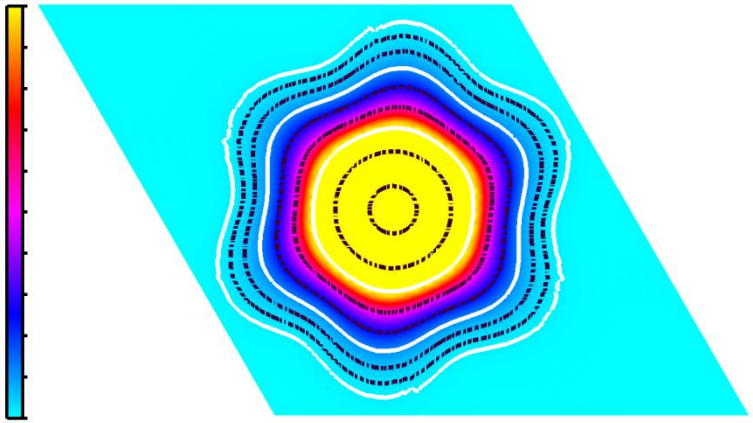

The calculated water charge density slices along the *ab*-plane at the positions of the proton (left) and oxygen (right) atoms. The contours represent isoenergy lines; the bounding box is (-0.18, 0.18) along the *a*- and *b*-axes. The min/max charge (abs.val.) in the color-bars are 0.0224/0.0985 Ha/Å^3 (a), and 0.0224/ 13.6546 Ha/Å^3 (b).

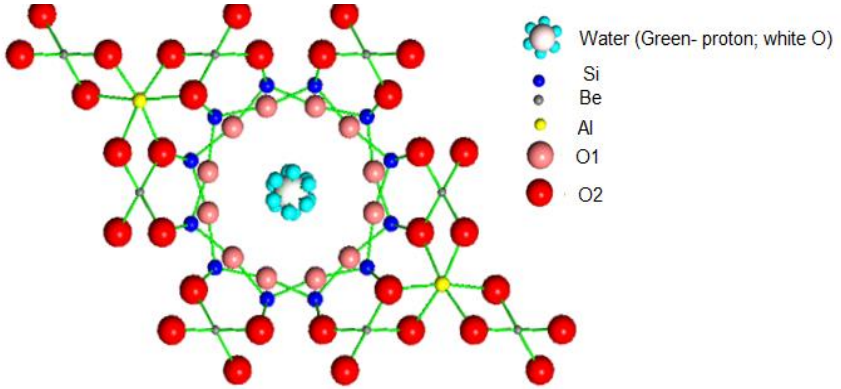

The DFT calculated structure of beryl well agrees with the experiment of Gatta *et al*., Am. Mineral. 91 (2006) 29.

$$H = -\frac{\hbar^2}{2I}\frac{\partial^2}{\partial\varphi^2} + \mathrm{V}(\varphi) \qquad \mathrm{V}(\varphi) = \frac{V_6}{2}(1 - \cos 6\varphi)$$

$$H_{nm} = \frac{\hbar^2 n^2}{2I}\delta_{n,m} + \frac{V_6}{4}\{2\delta_{n,m} - \delta_{n-m+6,0} - \delta_{n-m-6,0}\}, \quad n, m = 0, \pm 1, \pm 2, \ldots$$

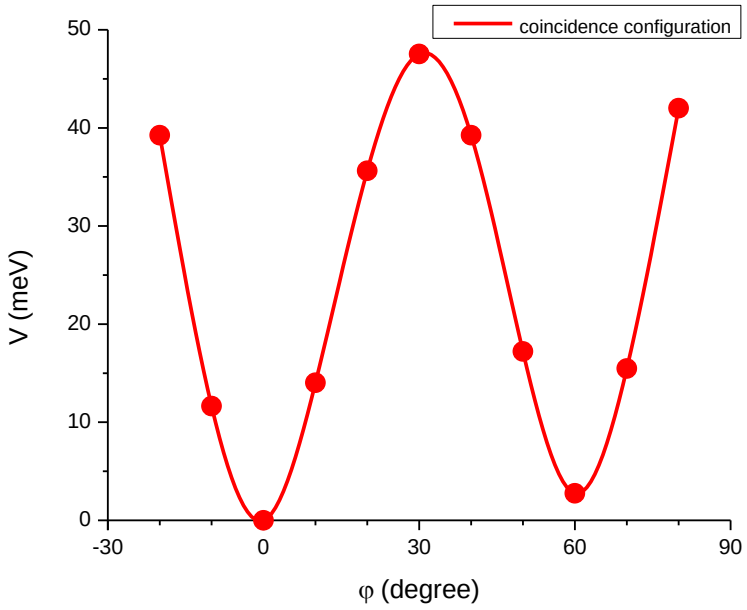

m	E_m (meV) V_6=48 meV	ΔE (meV) V_6=48 meV	Transitions (*m*=0)→(*m'*)
0	21.42		
1, 5	24.16	2.74	0→1, 0→5
2, 4	31.81	10.39	0→2, 0→4
3	38.73	17.31	0→3

Water enters SWNT by exposing them to water vapor at 110°C

Low-angle neutron diffraction: I(Q) ~ S(Q)•F(Q). Here, S(Q) consists of a Bragg reflection at 0.41 Å^{-1} from the (01) planes of the 2D hexagonal lattice of SWNT crystalline bundles.

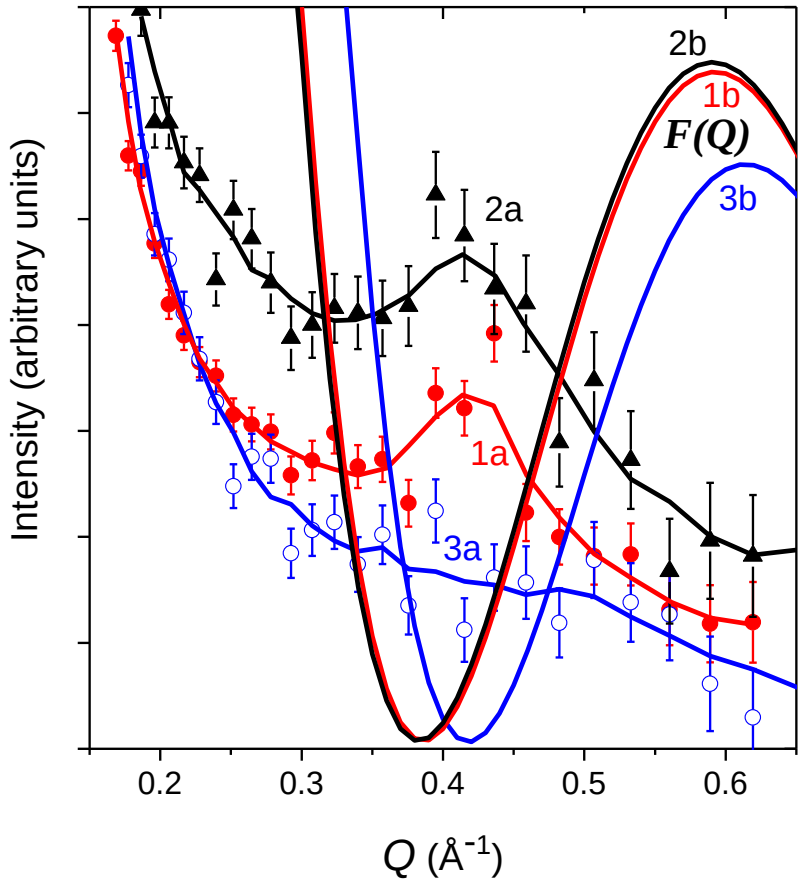

1 – Dry SWNT; 2 – SWNT & H_2O
3 – SWNT & D_2O

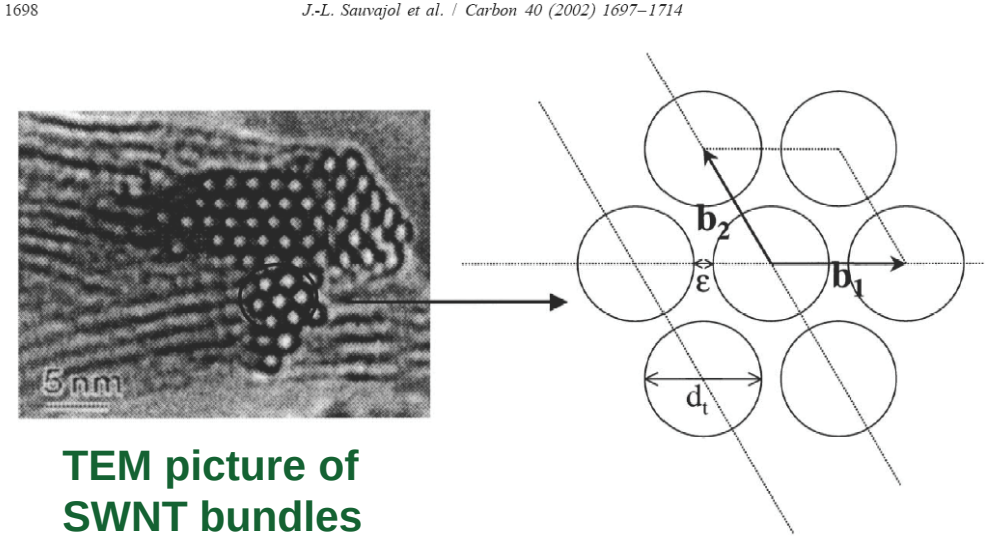

TEM picture of SWNT bundles

Fig. 1. Left: transmission electron microscopy observation of crystalline packing of SWNT in bundles (from Ref. [10]). Right: sketch of the 2D hexagonal lattice.

SWNT (D≈14±1 Å, l~10 μm) was characterized by HRTEM, TEM, SEM, Raman, ND.

To fill SWNT with water, the dry SWNT was exposed to water vapor at 110°C. The excess water in the exterior of the nanotubes was evaporated at 35°C. An optimal filling, H_2O/SWNT mass ratio, was found to be 11%.

Water in SWNT and pressure effect

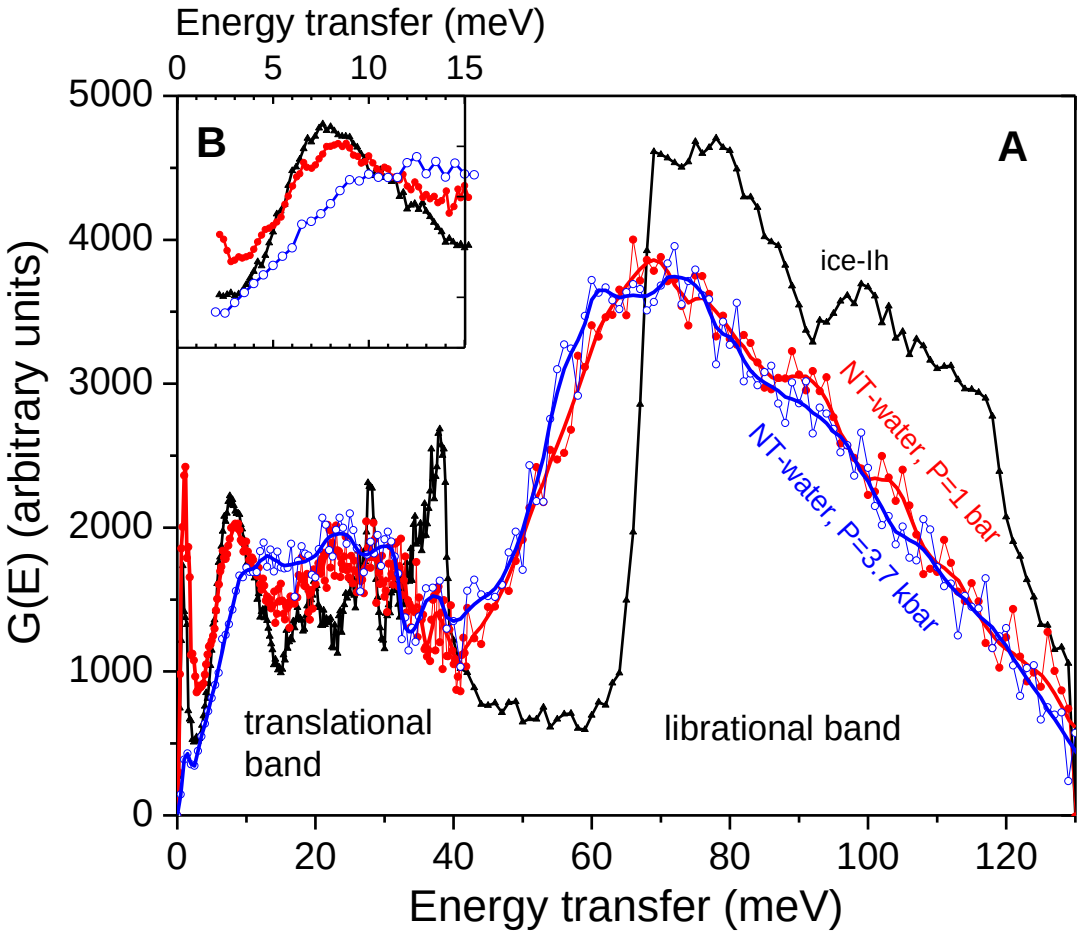

Pressure effect

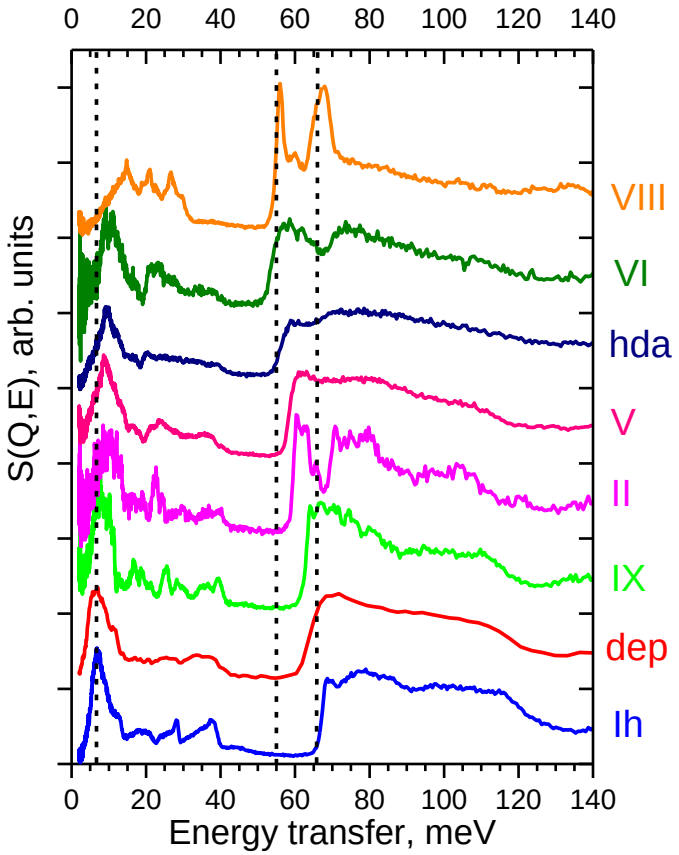

INS spectra of different phases of bulk ice

A Weak Hydrogen-Bond Network in Nanotube-Water

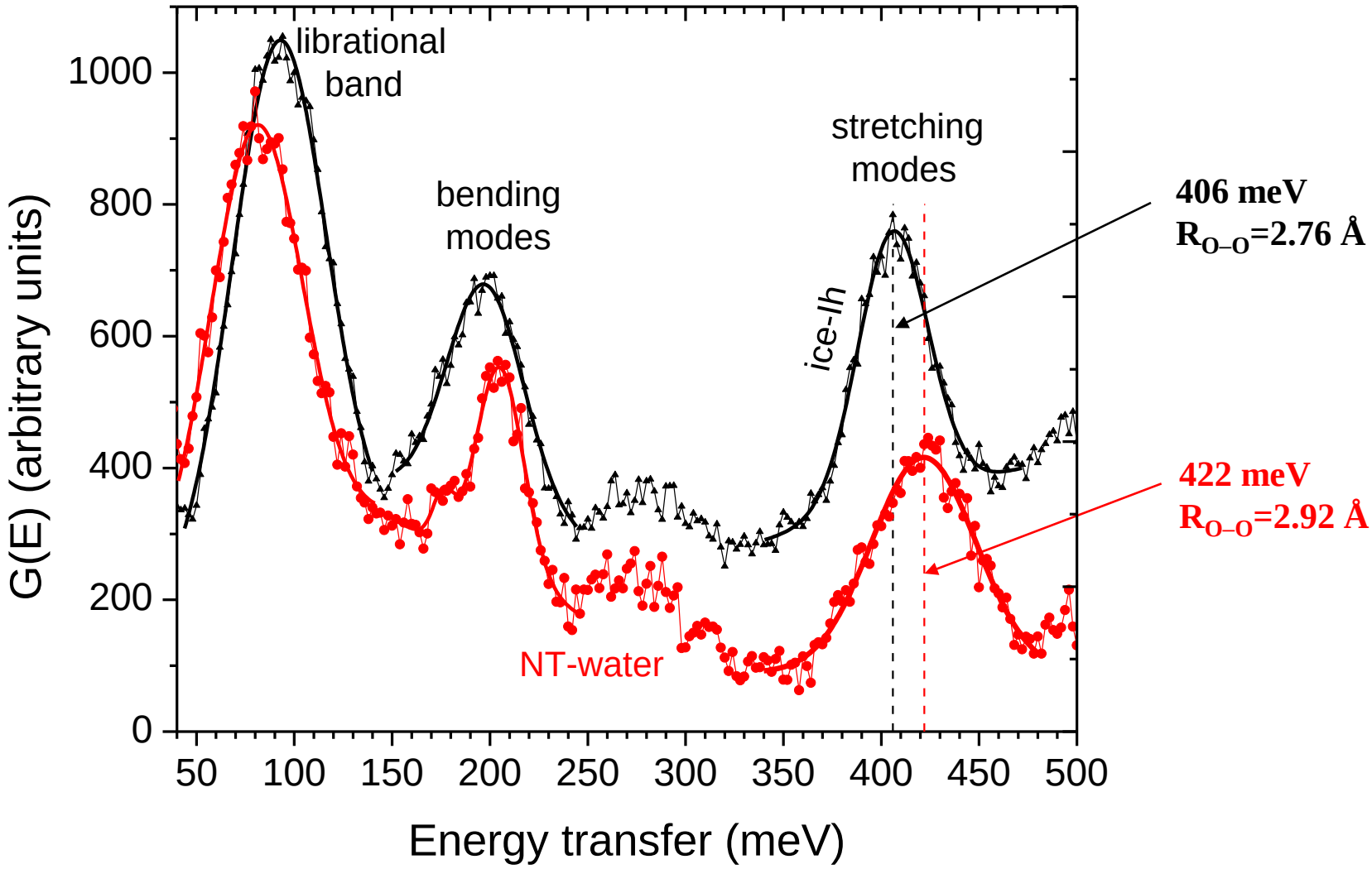

Pressure effect on the calculated structure and vibrational spectra of nanotube-water at T=100 K.

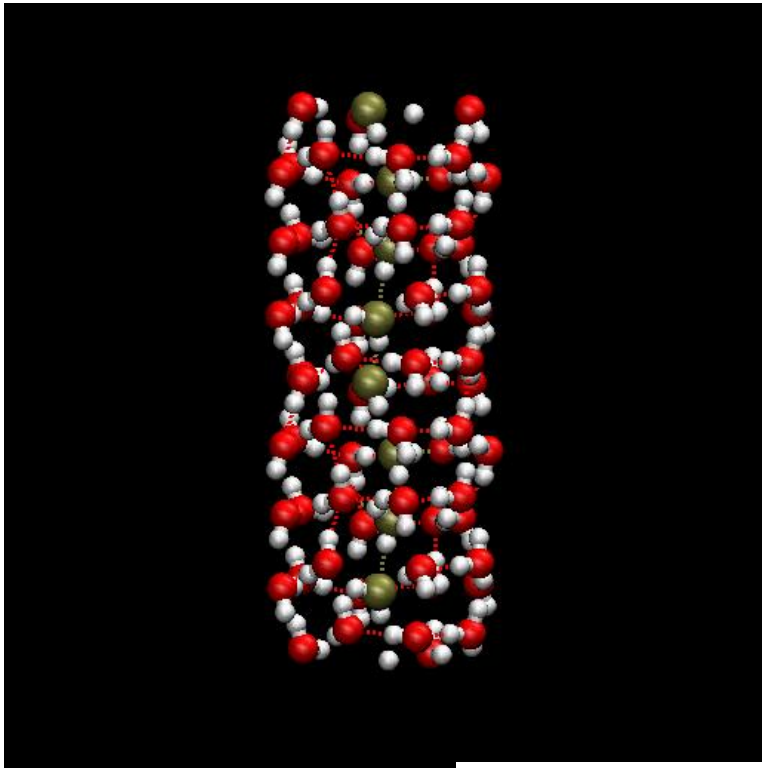

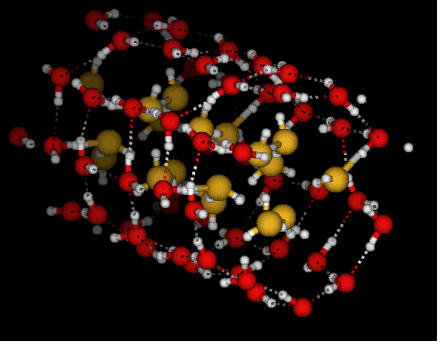

Proposed structure of high pressure nanotube-water

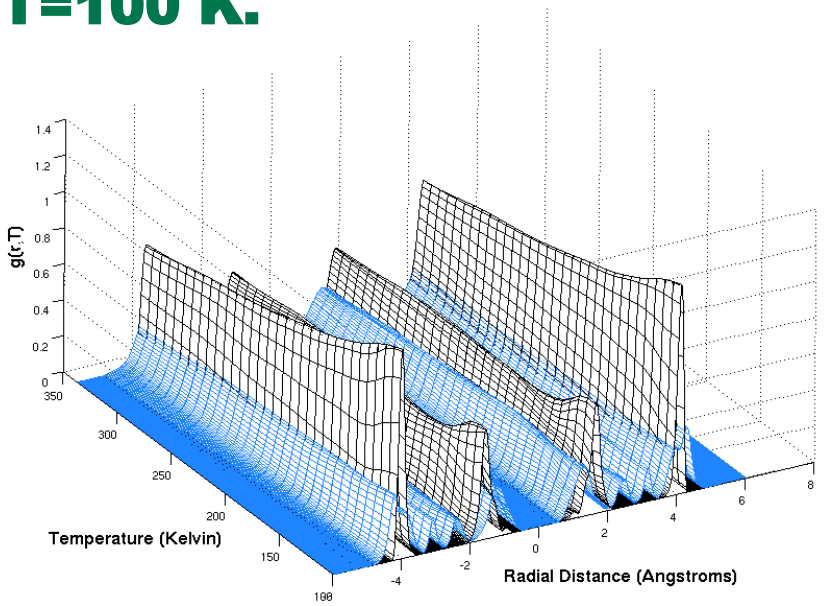

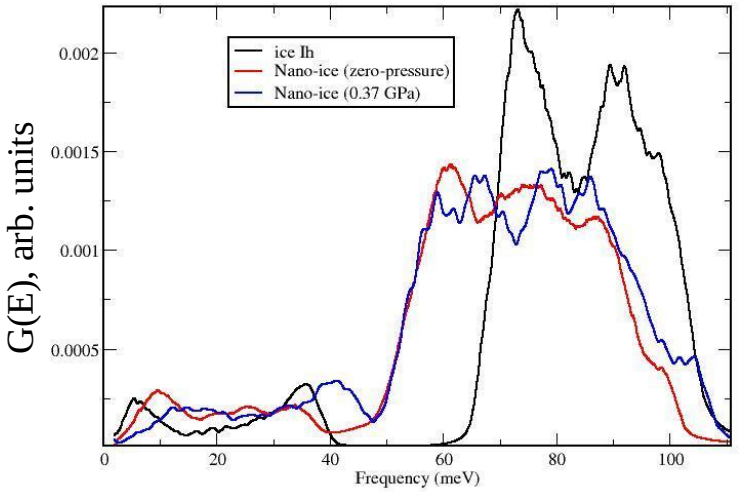

Calculated vibrational spectra for nanotube-water at P=1 bar and P=3.7 kbar, compared to ice-Ih

Inelastic neutron scattering (INS) is one of a preferred method to study the dynamics of hydrogen containing materials owing to the extraordinarily large scattering cross-section of hydrogen and the straightforward comparison of the experimental data with the results of model simulations.

$$S(Q,E) = \sum_{l,k} \sigma_H^{inc} \exp(-2W(Q)) \left(\frac{\hbar Q^2}{6M}\right)^k \int d\omega_1 ... d\omega_k \frac{G(\omega_1)...G(\omega_k)}{\omega_1 ... \omega_k (k-l)! l!} \prod_{i=l+1}^{k} [n_B(\omega_i, T) + 1] \prod_{j=1}^{l} n_B(\omega_j, T) \delta(E - \sum_{i=l+1}^{k} \hbar\omega_i + \sum_{j=1}^{l} \hbar\omega_j)$$

$$S_{1ph}(Q,\omega) = \sigma_H^{inc} \frac{\hbar Q^2}{2M} \exp(-2W(Q)) \frac{G(\omega)}{\omega} [n_B(\omega, T) + 1]$$

where

$$W = \frac{1}{2} < (\mathbf{Qu})^2 > = \frac{\hbar Q^2}{2M} \int \frac{G(\omega)}{\omega} [2n_B(\omega, T) + 1] d\omega$$

and *G(ω)* can be calculated as

$$G(\omega) = \sum_{j,\mathbf{q}} \frac{1}{3N} |\mathbf{e}(j,\mathbf{q})|^2 \delta[\omega - \omega(j,\mathbf{q})]$$

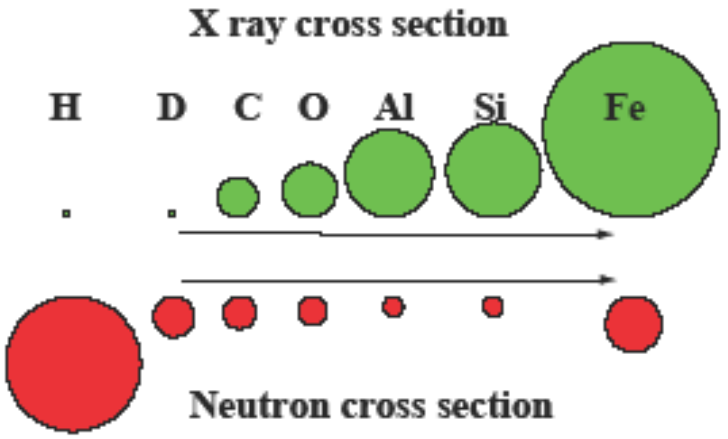

Quantum rotation of ortho- and para-water encapsulated in a fullerene cage

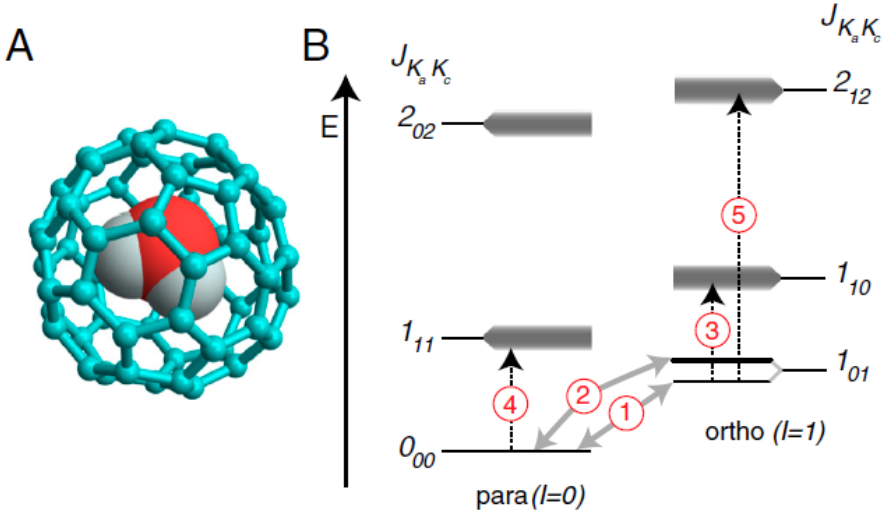

Fig. 1. (*A*) Molecular structure of the water-endofullerene $H_2O@C_{60}$, using a ball-and-stick representation for the C_{60} cage and space-filling spheres for water; (*B*) Energy level diagram, showing the principal transitions detected by INS (grey arrows) and IR spectroscopy (dashed arrows). The three-fold rotational degeneracy of the *ortho*-H_2O ground state is lifted. The upper level of the split 1_{01} state is doubly degenerate. Unresolved fine structure is indicated by shading.

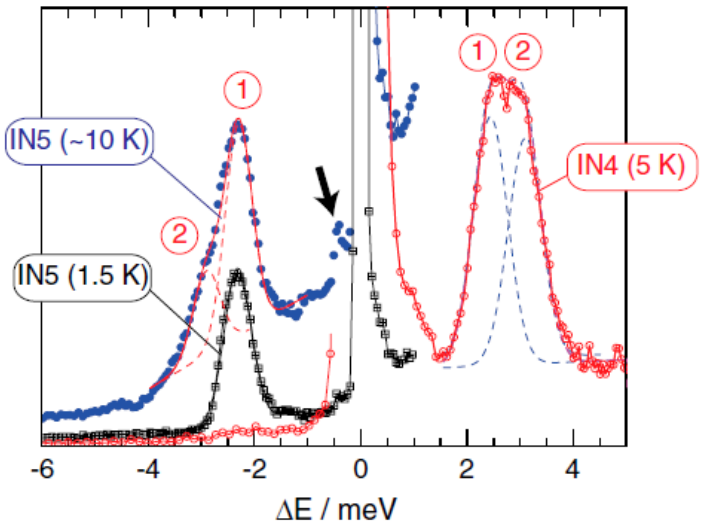

Fig. 2. INS spectra recorded on the time-of-flight spectrometers IN4 and IN5. The 10 K spectrum is an average over 5, 10, and 15 K data. The dashed lines show the best fit components where the transitions are labeled according to Fig. 1*B*.

Carlo Beduz[a], Marina Carravetta[b], Judy Y.-C. Chen[c], Maria Concistrè[b], Mark Denning[b], Michael Frunzi[c], Anthony J. Horsewill[d], Ole G. Johannessen[b], Ronald Lawler[e], Xuegong Lei[c], Malcolm H. Levitt[b,1], Yongjun Li[c], Salvatore Mamone[b], Yasujiro Murata[f], Urmas Nagel[g], Tomoko Nishida[f], Jacques Ollivier[h], Stéphane Rols[h], Toomas Rõõm[g], Riddhiman Sarkar[b], Nicholas J. Turro[c], and Yifeng Yang[a]

[a]School of Engineering, University of Southampton, Southampton SO17 1BJ, United Kingdom; [b]Chemistry, University of Southampton, Southampton SO17 1BJ, United Kingdom; [c]Department of Chemistry, Columbia University, New York, NY 10027; [d]School of Physics and Astronomy, University of Nottingham, Nottingham NG7 2RD, United Kingdom; [e]Department of Chemistry, Brown University, Providence, RI 02912; [f]Institute for Chemical Research, Kyoto University, Uji, Kyoto 611-0011, Japan; [g]National Institute of Chemical Physics and Biophysics, Akadeemia tee 23, Tallinn 12618, Estonia; and [h]Institut Laue-Langevin, BP 156, 38042 Grenoble, France

PNAS 109 (2012) 12894

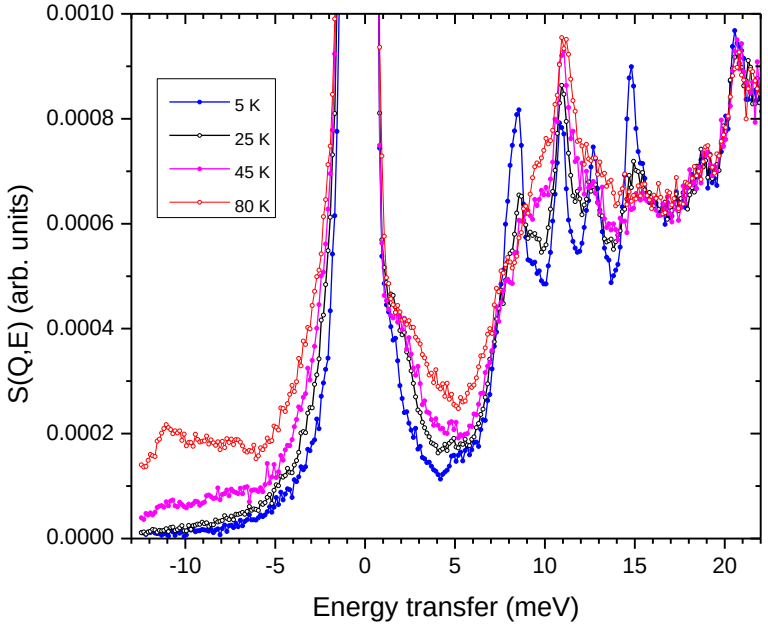

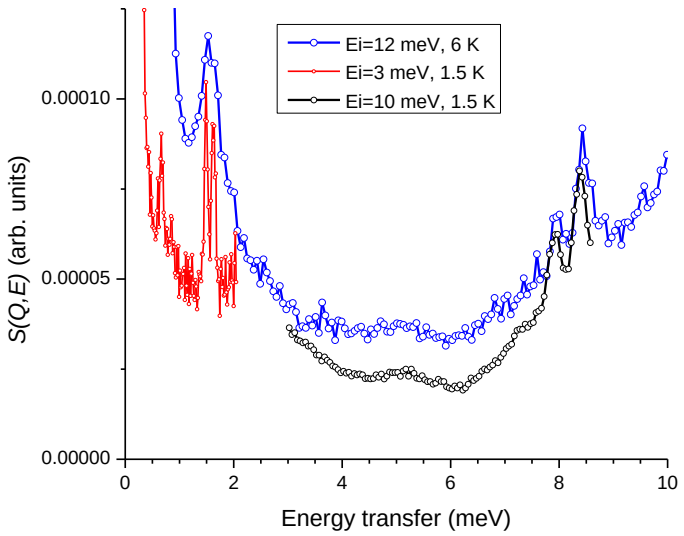

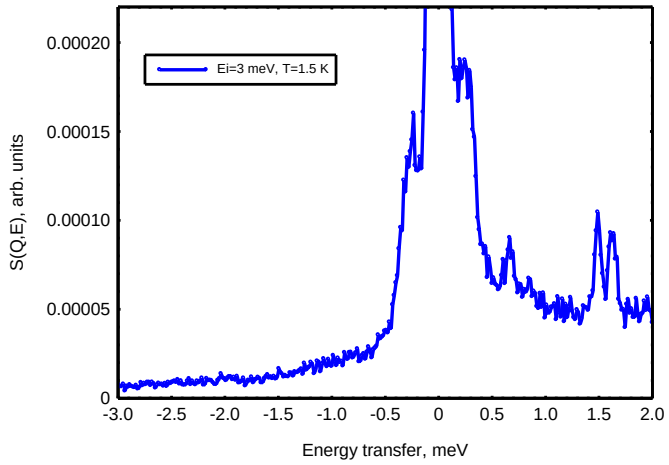

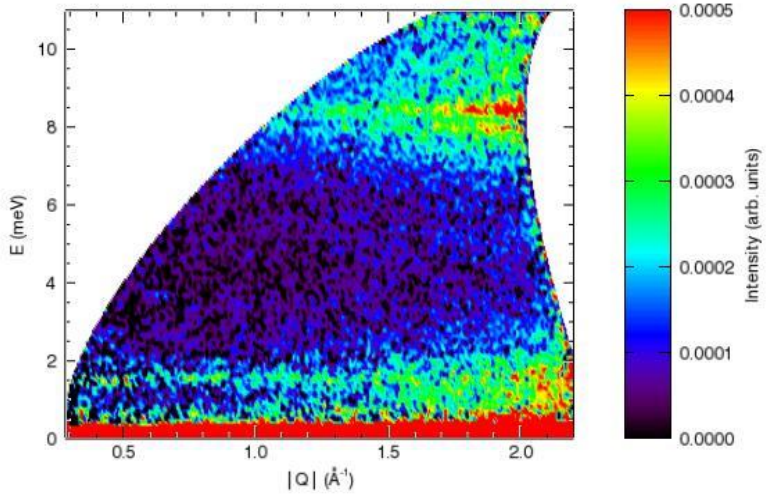

No para-ortho transitions of water in beryl were observed, probably water in beryl is not as free as water in fullerene.

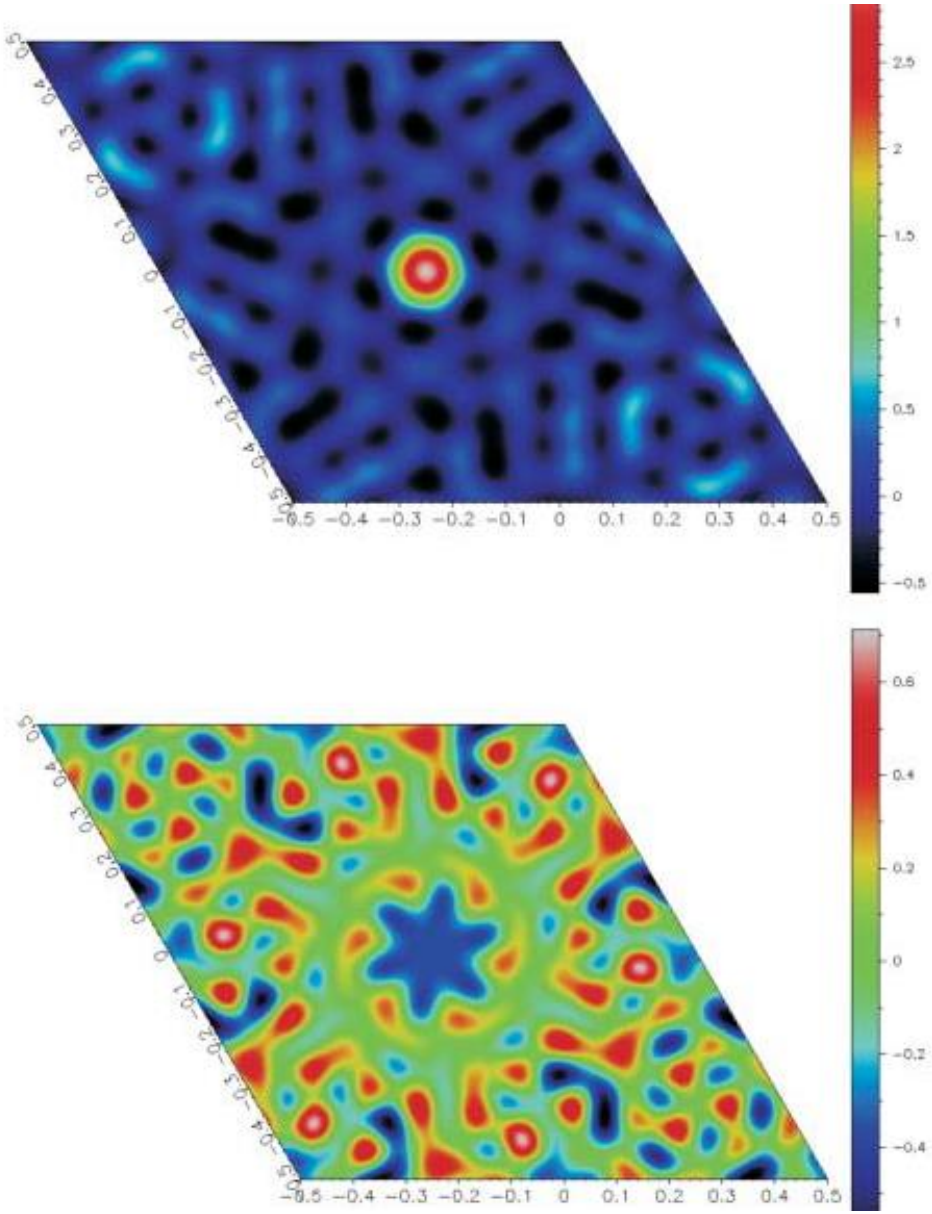

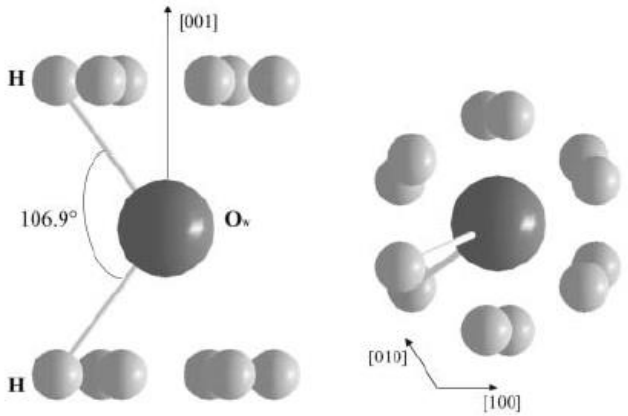

Topological configuration of water molecules into the channel of the alkali-poor beryl, viewed down [100] (left) and down [001] (right).

G.D. Gatta *et al*., Am. Mineral. 91 (2006) 29.

FIGURE 2. Difference-Fourier maps of the nuclear density of beryl at $z = 0.25$ (above) and $z = 0.332$ (below) after the first cycles of isotropic refinement with a channel-free structure. At $z = 0.25$ a residual peak of about +2.9 fm/Å^3 is seen lying on the sixfold axis, whereas at $z = 0.332$ there are six negative residual peaks (with a star shaped distribution) of about –0.6 fm/Å^3 around the sixfold axes. Note that the color scale is different for the two maps.

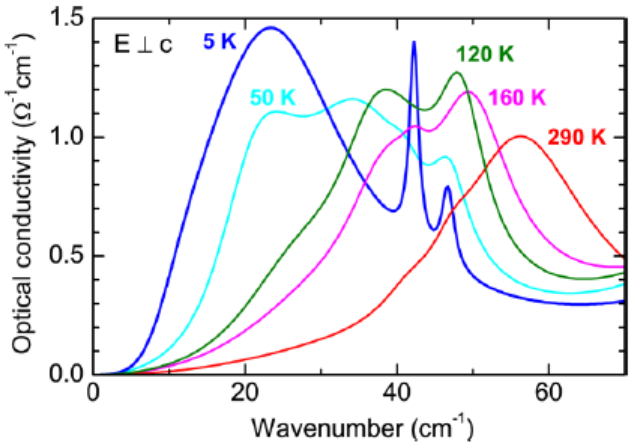

Figure 5. THz conductivity due to water absorption in beryl measu
for radiation polarized perpendicular to the axis of the nanopore
different temperatures, as indicated.

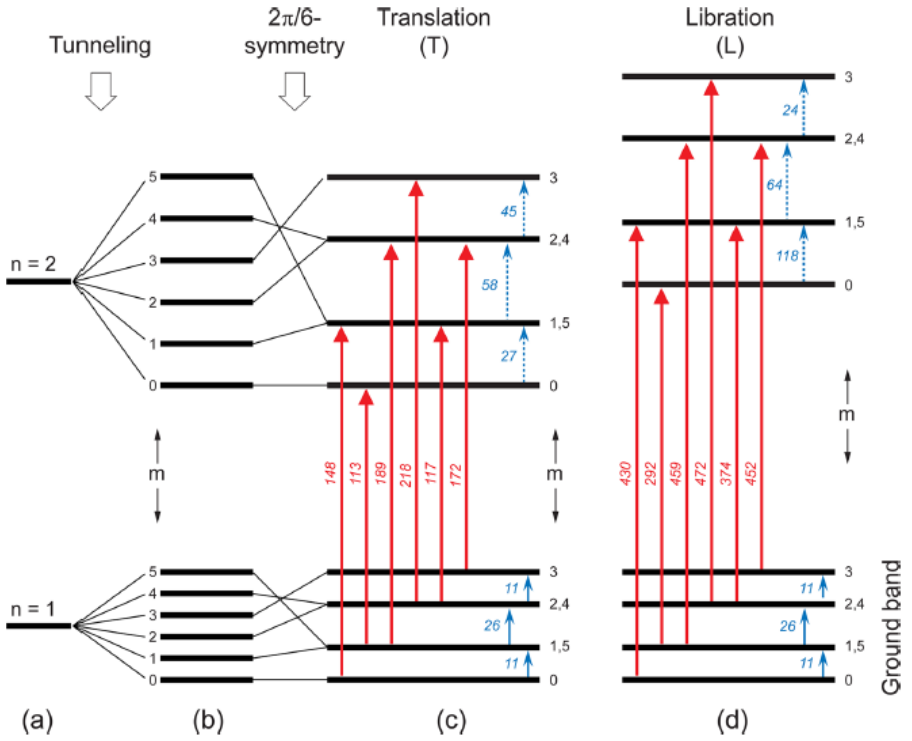

Figure 4. Scheme of vibronic energy levels of a type-I water molecule in a nanocavity of the beryl crystal lattice. The lowest-energy bands are shown. (a) Ground state ($n = 1$) and first excited in-plane vibrational state ($n = 2$) for small vibrations around a preferred direction. (b) Due to tunneling within the six-well potential, the states split according to their angular quantum number m. Two couples are degenerate, $m = 1$ and $m = -1 = 5$, and also $m = 2$ and $m = -2 = 4$ due to the six-fold symmetry. (c,d) The long red arrows indicate interband transitions, while the short blue arrows correspond to optical transitions within one band. The selection rule $\Delta m = \pm 1$ allows only certain transitions. The dotted arrows correspond to transitions that are not seen in our experiment. The corresponding frequencies are given in units of cm^{-1}, where 100 cm^{-1} corresponds to 12 meV or 3 THz.

The tunnel splitting of water vibrational states in beryl were predicted in [1], where the authors used optical spectroscopy. The positions of the observed optical peaks assigned to intra-ground-band transitions with energies 1.33, 3.21, 5.21 and 5.82 meV disagree with our INS data, where isotropic tunneling peaks were observed at 0.66, 1.49 and 1.63 meV, and anisotropic peaks at 0.27, 7.9 & 8.4, 12.7 and 14.7 meV, which were visible only for Q⊥c-axis.

[1] Gorshunov *et al*., J. Phys. Chem. Lett. 4 (2013) 2015

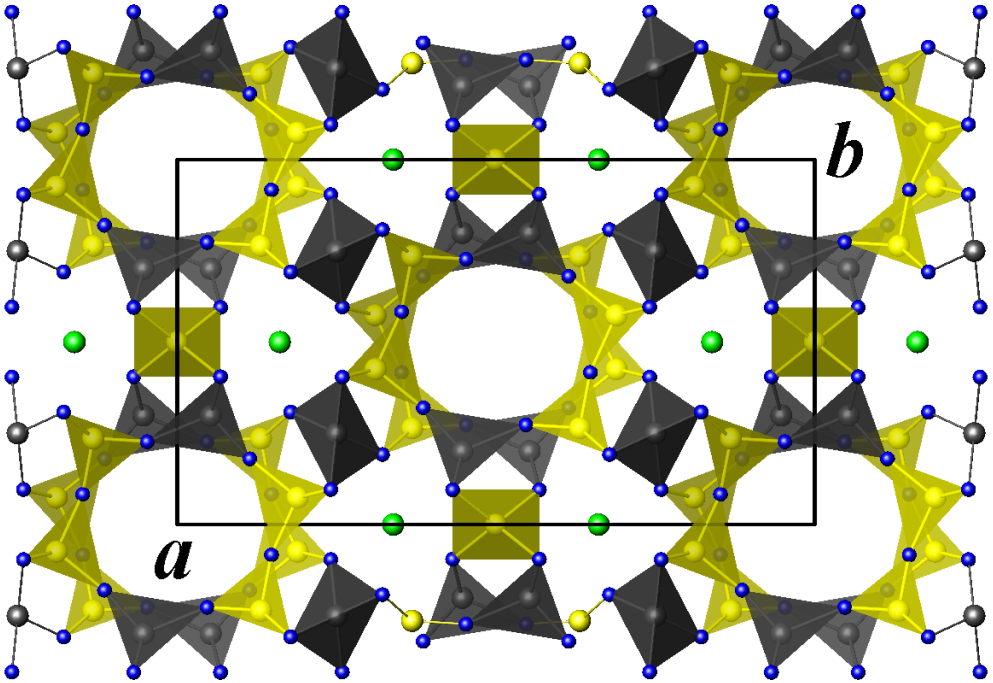

Structure of cordierite ($Al_4Mg_2Si_5O_{18}$) showing large open channels running parallel to the crystallographic *c*-axis (out of the figure's plane): Si, yellow; Al, blue; O, red; and Be, green.

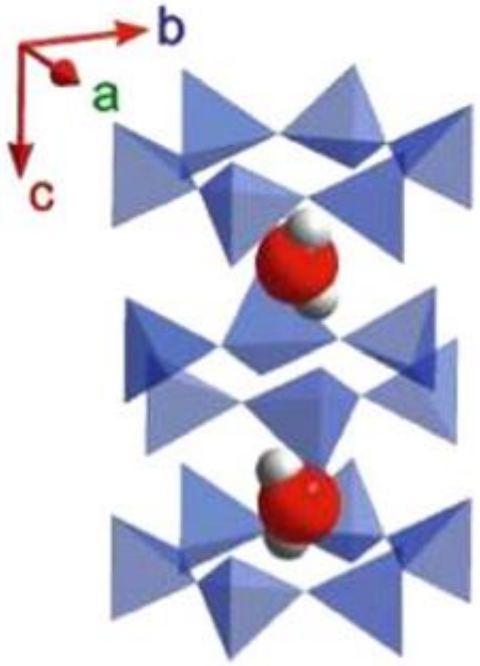

Graphical representation of the alignment of water molecules inside the channels of cordierite.

S(Q,E) spectra, SEQUOIA

Beryl, Q∥c

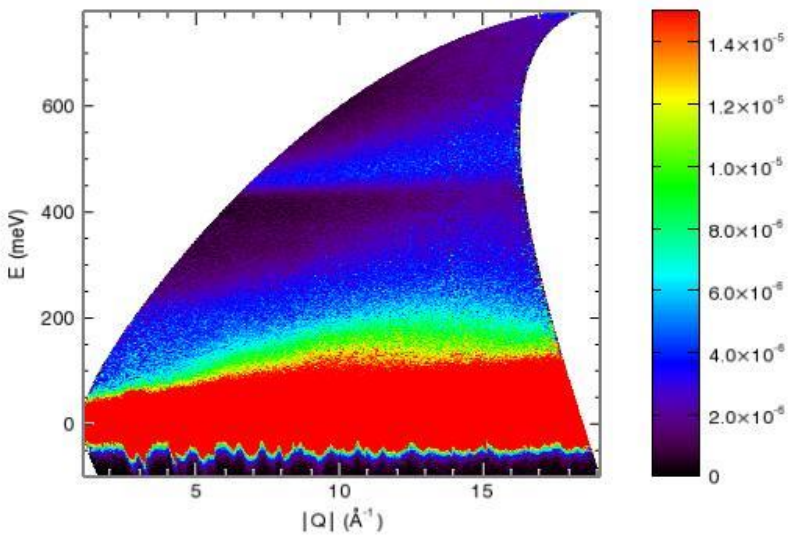

Cordierite, Q∥c

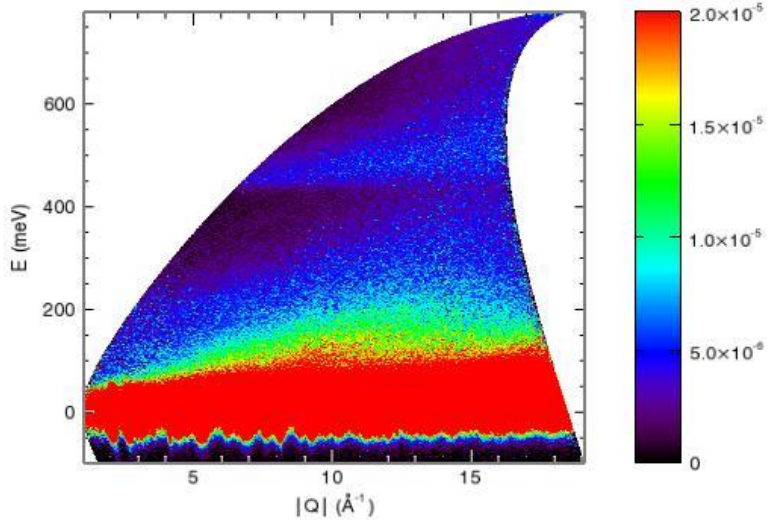

Beryl, Q⊥c

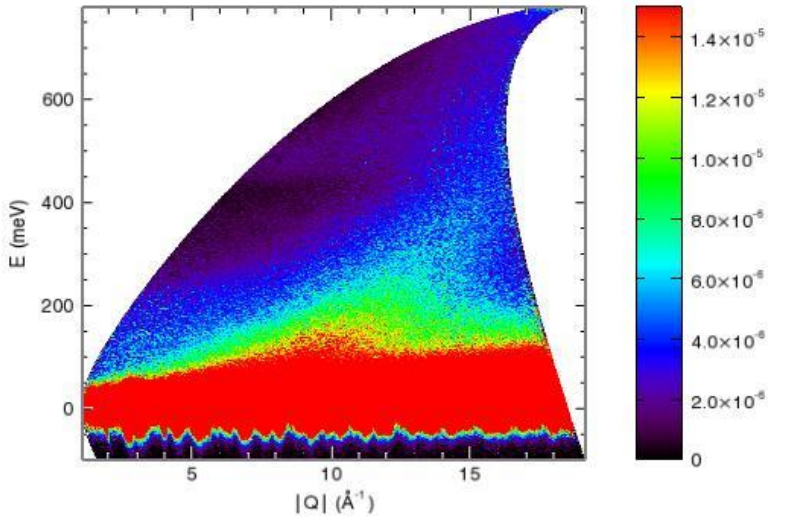

Cordierite, Q⊥c

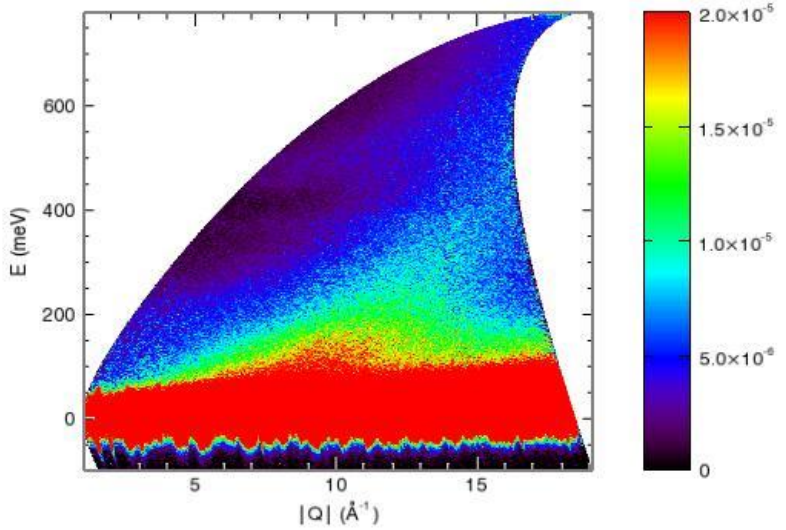

Beryl

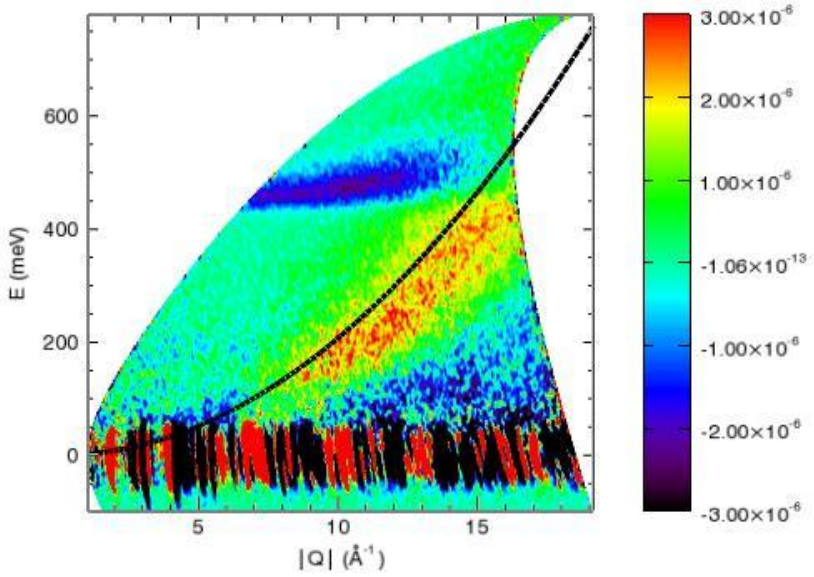

Cordierite

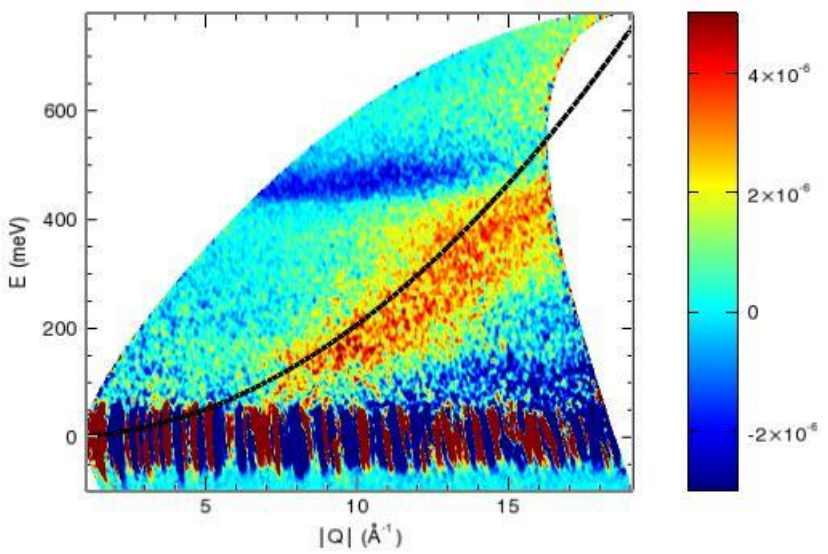

Difference between the S(Q,E) spectra for $Q_{\perp}c$ and $Q\|c$ orientations. The solid lines show the neutron recoil spectra for free particles of mass *m*=1 a.u., $E=\hbar^2Q^2/2m$.

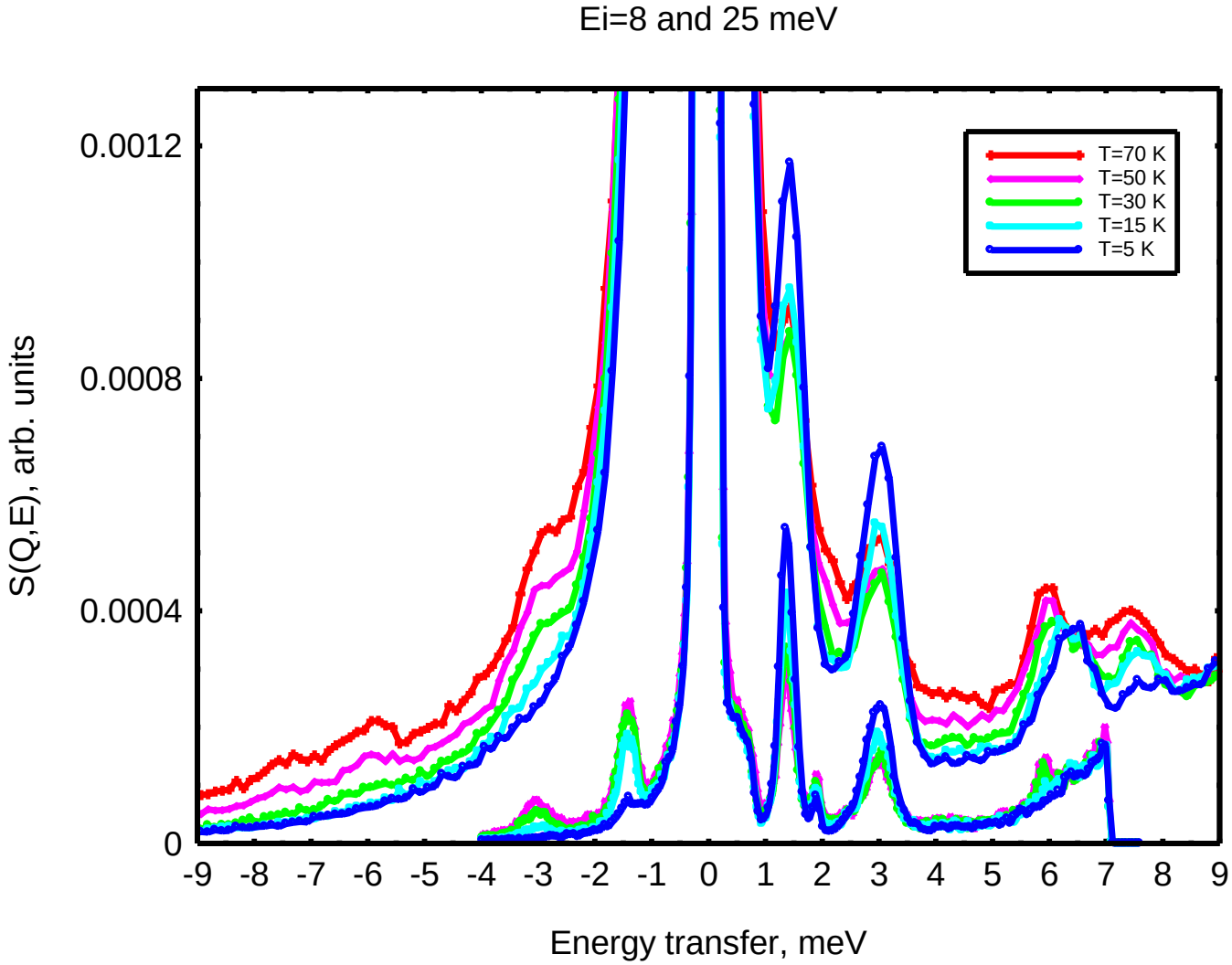

The peaks at 1.4 and 3.0 meV are due to transitions between the levels of the ground state of iron atoms impurity, which are split due to crystal field effect. The intensity of these peaks at energy loss side decrease with temperature increase.

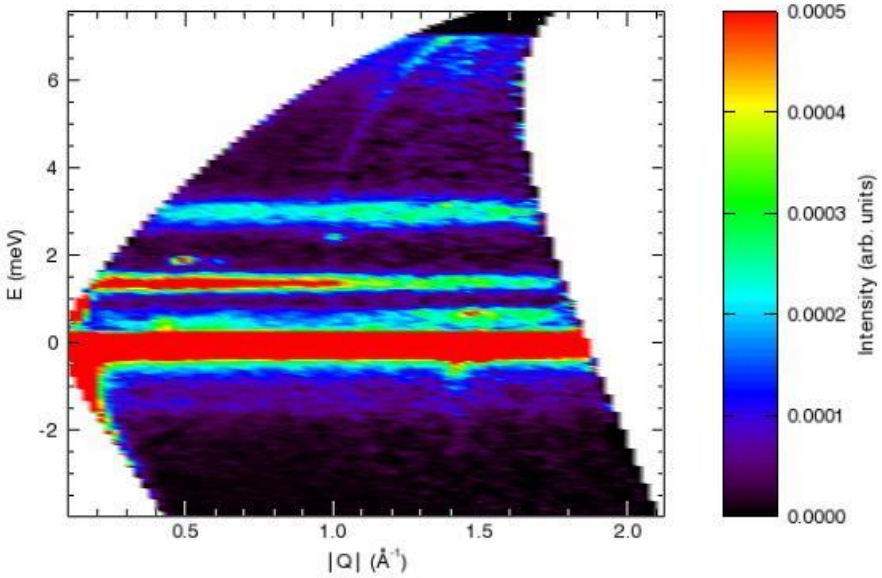

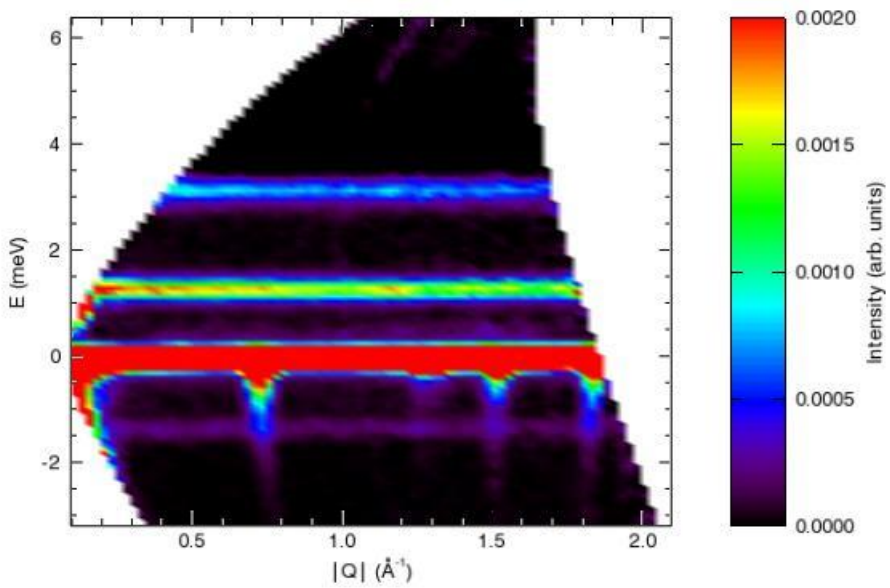

Cordierite and dry cordierite, E_i=8 meV, T=5 K

The water librational vibrations in beryl have a broad peak at relatively low energy, E_{lib}≈22 meV (the INS result), and for simplified model of 1D harmonic rotational oscillator, the kinetic energy of water proton in the ground state can be estimated as E_k=E_{lib}/4=5.5 meV. The De Broglie wavelength, $\lambda = \frac{h}{Mv} = \frac{h}{\sqrt{2ME_k}}$ ≈3.8 Å for this quasi-1D proton (with only one rotational degree of freedom) is much larger than the distances between the proton's possible positions in the cage, which are about 0.6, 1.04 and 1.2 Å, therefore proton in this state might experience quantum tunnel between them, resulting in multiple splitting of its ground state. The splitting of the water proton ground state due to its tunneling can be roughly estimated by using approximate formula [1] for the particle in harmonic double-well potential with minima separated by *l*=0.6 Å

$$\Delta E_{tun} \approx \frac{E_{lib}}{2} exp(-\frac{ME_{lib}l^2}{\hbar^2})$$

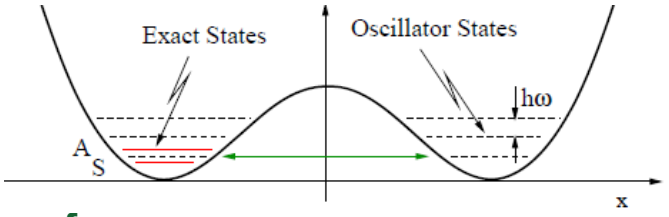

which gives a value (~7 meV) comparable to the energies of the observed tunneling peaks.

[1] S.L. Drechsler *et al*. J. Phys. F: Met. Phys. 14 (1984) L243

INS spectra of different ice phases

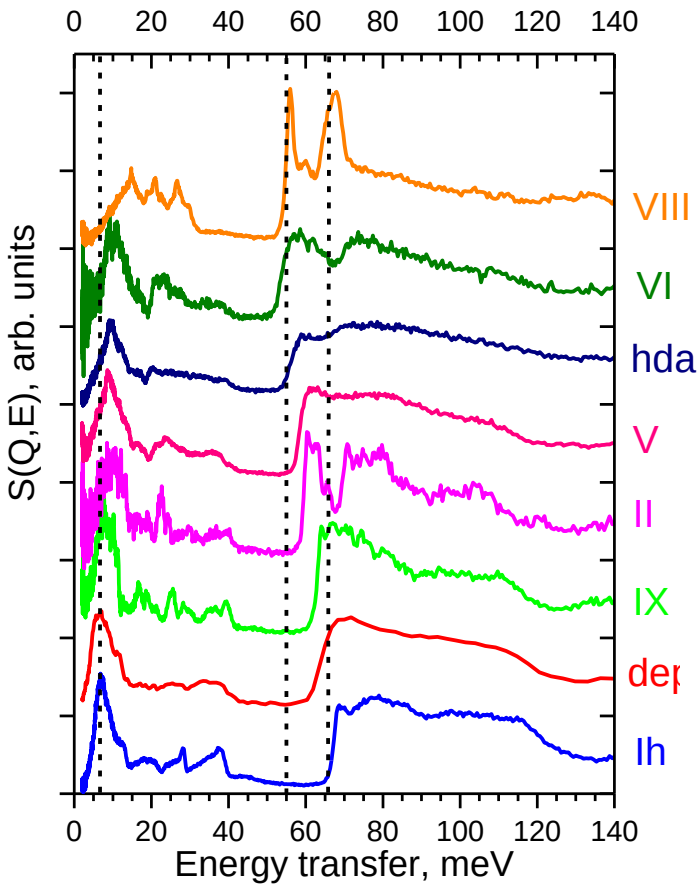

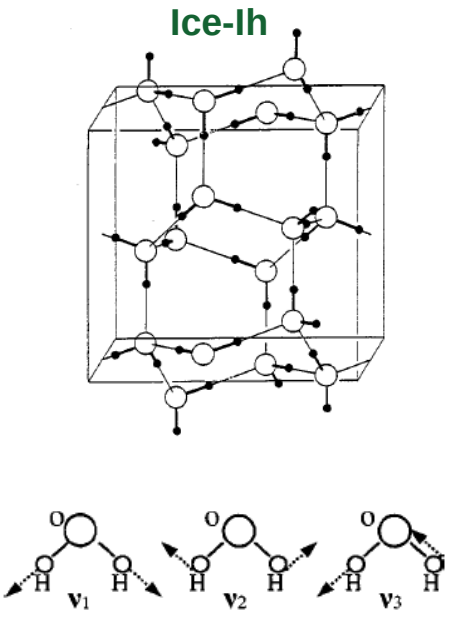

Schematic illustration of the bending and stretching modes in water molecule.

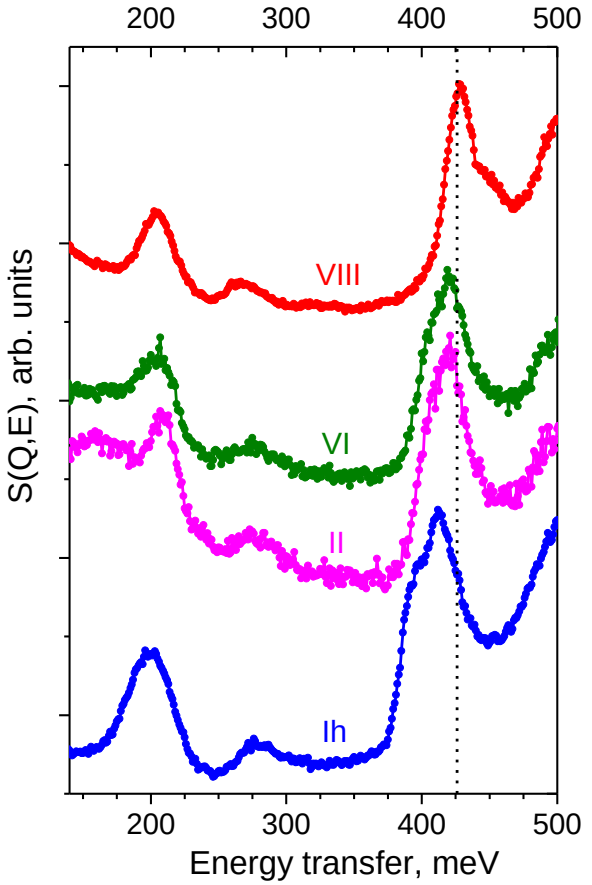

INS spectra of water in beryl, E_i=25 meV, measured at different temperatures

Q||*c*

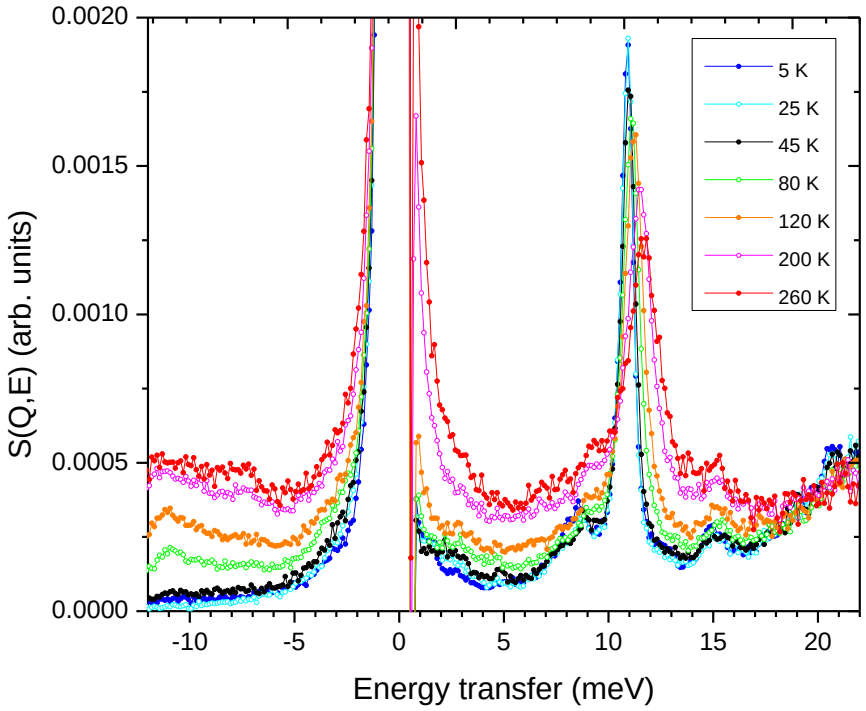

Q⊥*c*

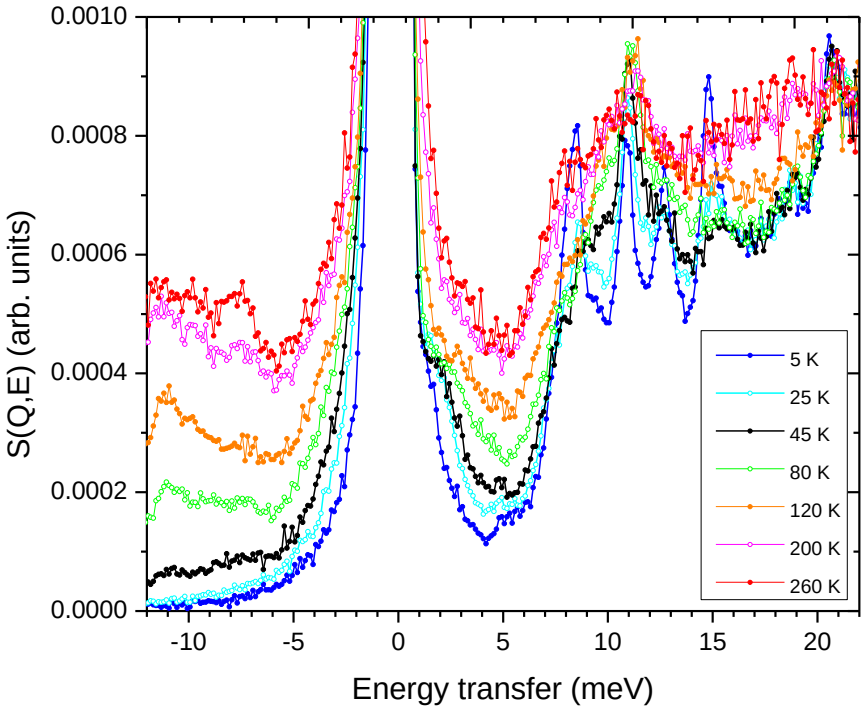

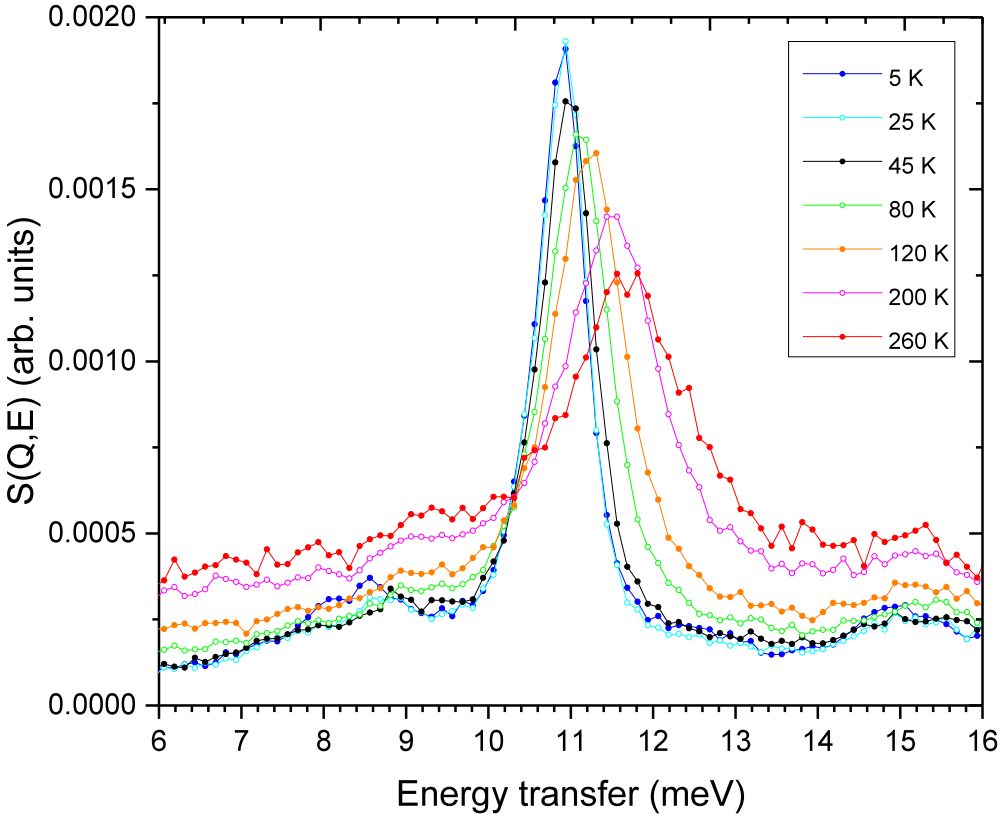

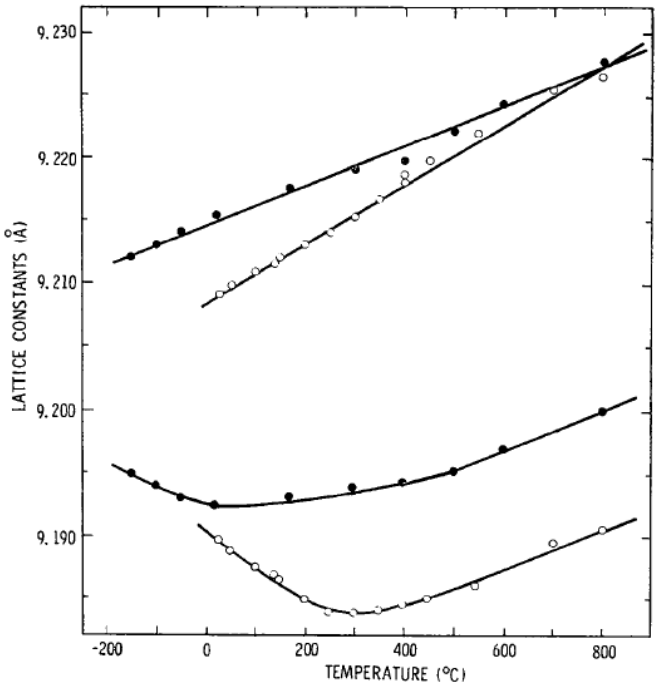

Lattice constants as a function of temperature for beryl and emerald. The values for beryl are shown as open circles, for emerald as solid circles. Note that both crystals exhibit a negative thermal expansion along the *c*-axis. B. Morosin, *Acta Cryst*. B28 (1972) 1899.

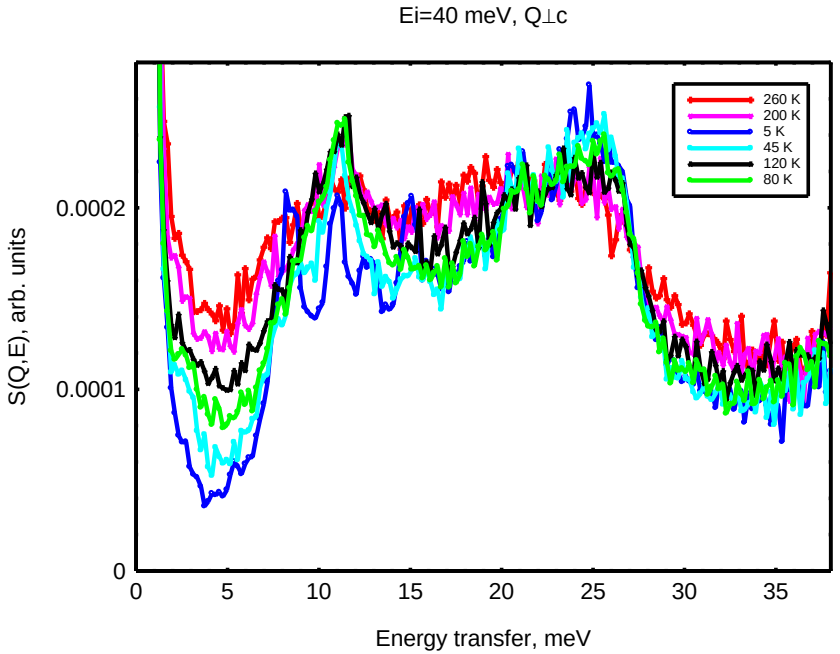

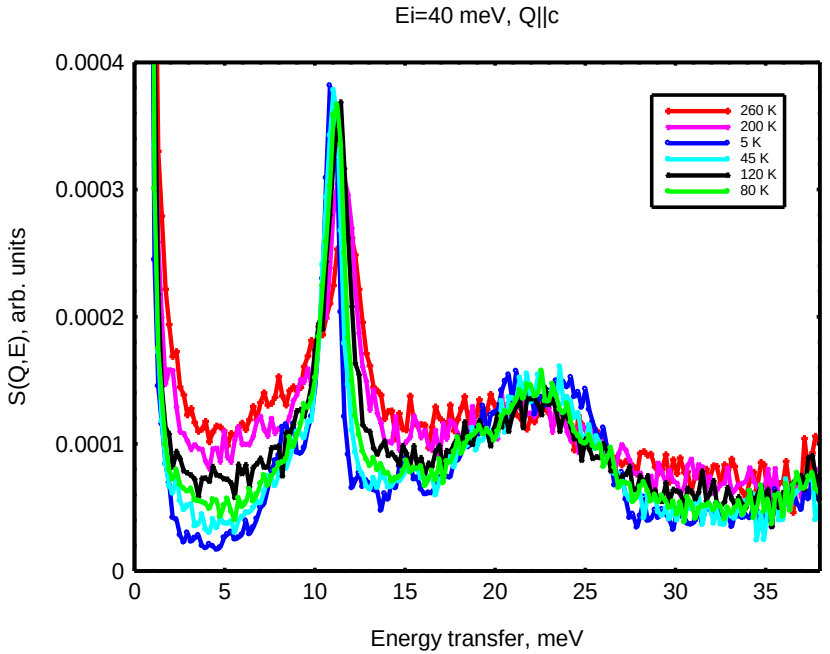

Temperature dependence of INS spectra for water in beryl measured with E_i=40 meV for Q||*c*-axis (left) and Q⊥*c*-axis (right) orientations.

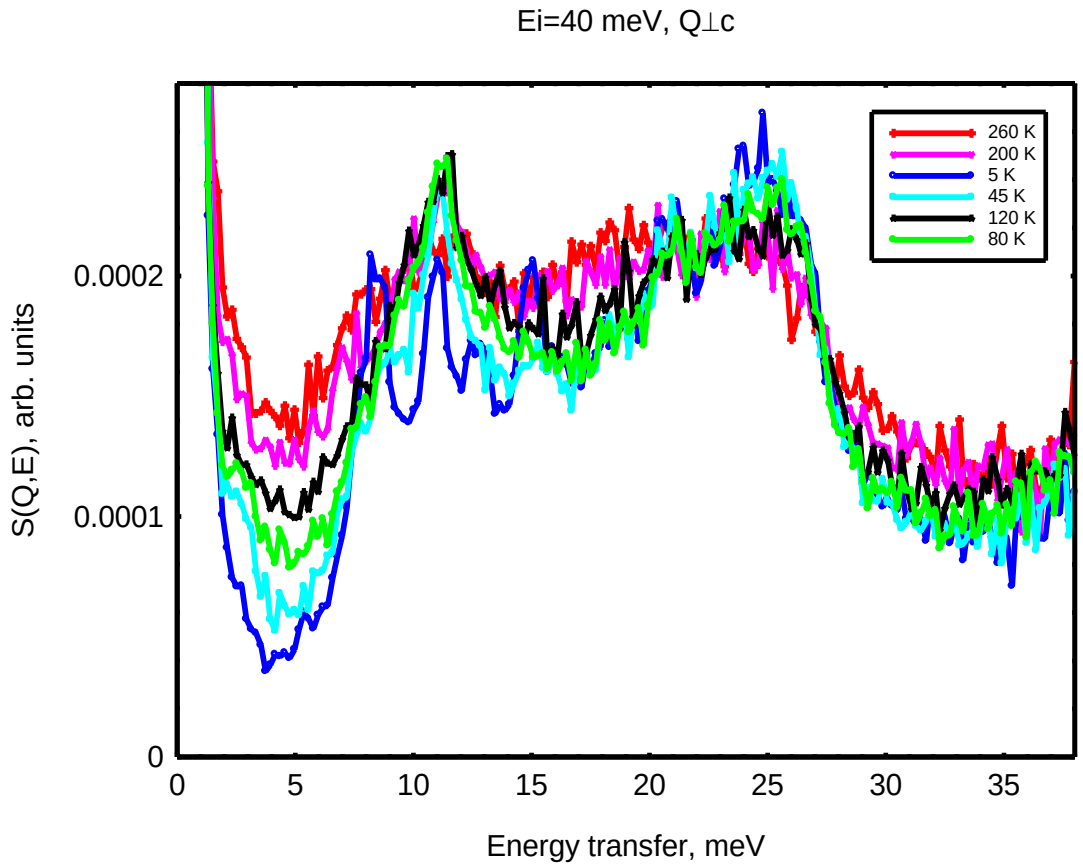
Ei=40 meV, Q⊥c
260 K
200 K
5 K
45 K
120 K
80 K
S(Q,E), arb. units
0.0002
0.0001
0
0
5
10
15
20
25
30
35
Energy transfer, meV

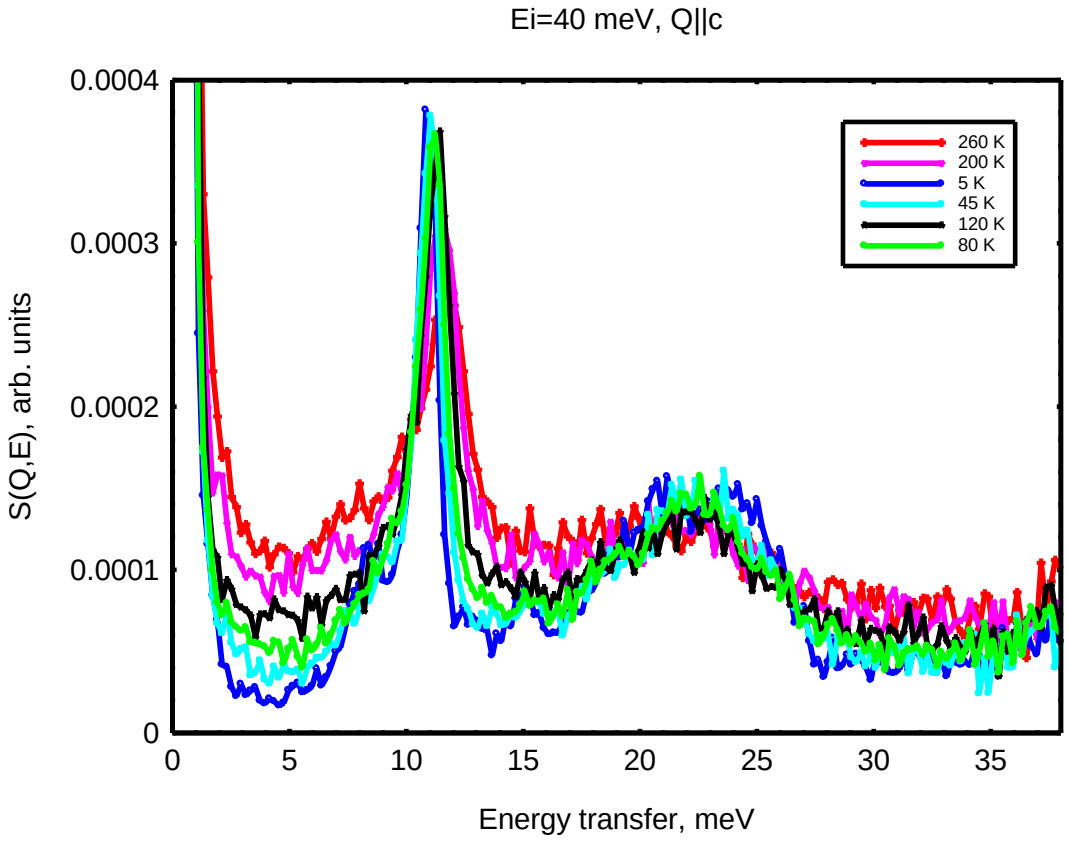
Ei=40 meV, Q||c
S(Q,E), arb. units
Energy transfer, meV
0.0004
0.0003
0.0002
0.0001
0
0
5
10
15
20
25
30
35
260 K
200 K
5 K
45 K
120 K
80 K

Q∥c

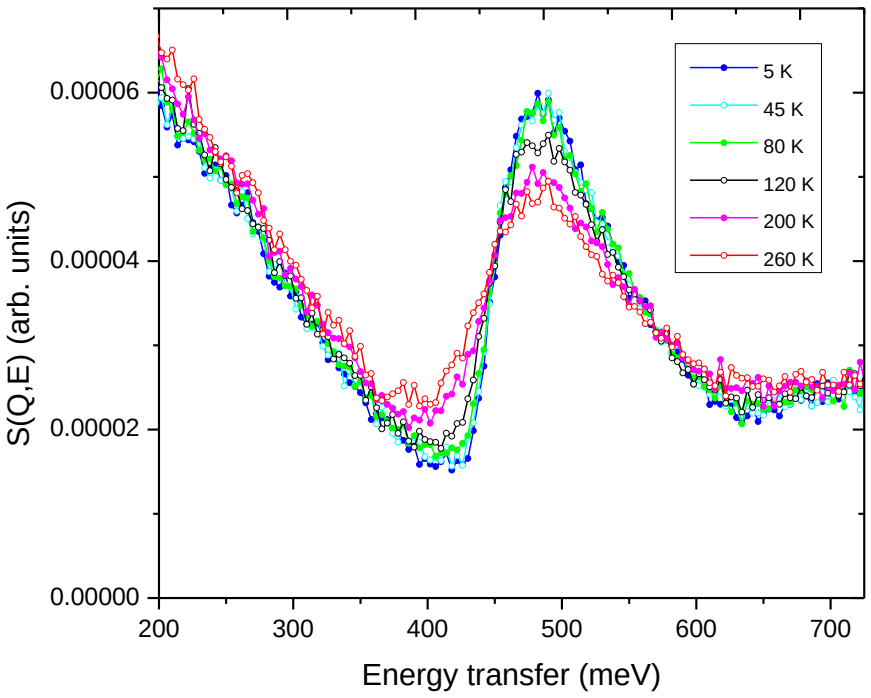

Q⊥c

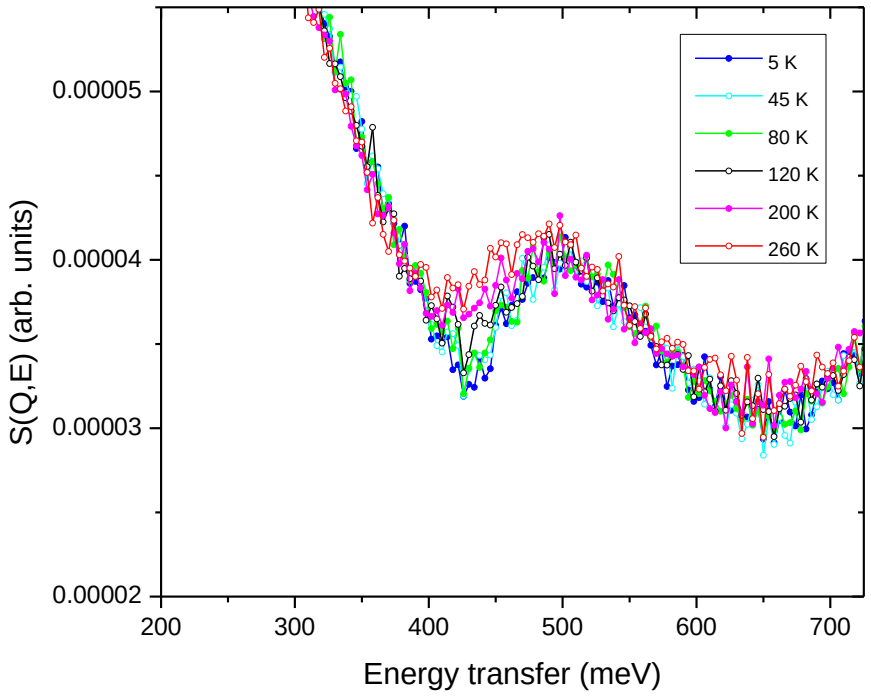

INS spectra of beryl showing softening of the water stretching O-H modes with temperature increase; E_i=800 meV.

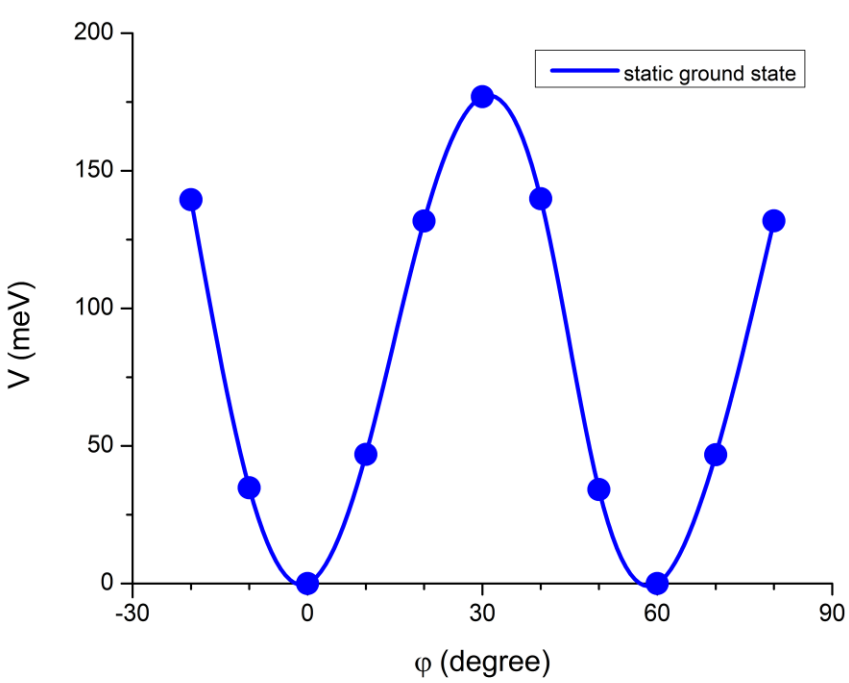

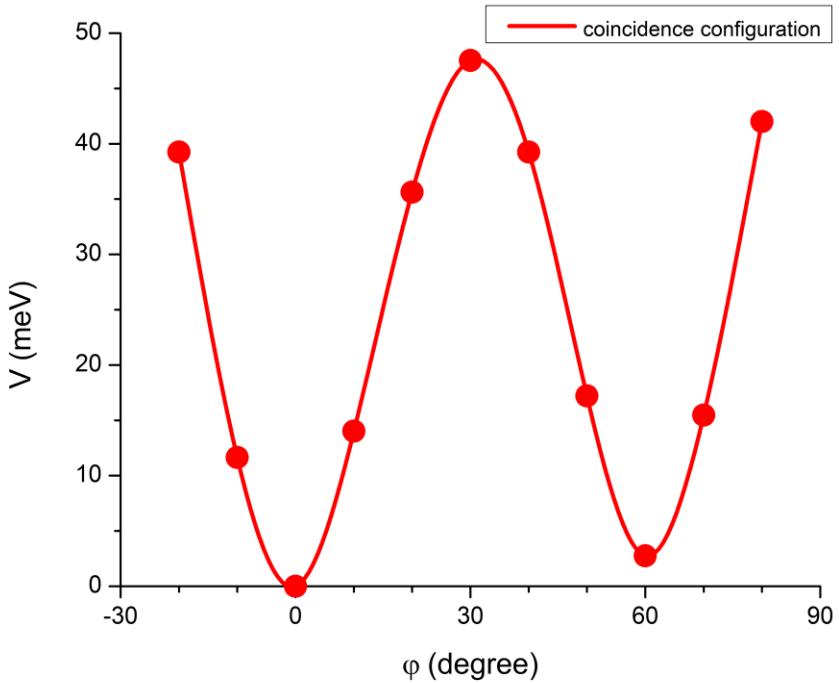

(a) The *ab initio* DFT calculated potential for rotation of water molecules about the *c*-axis starting from a static ground state equilibrium structure. The beryl lattice was allowed to relax, and quantum fluctuations were neglected in the DFT calculations. (b) The computed potential for rotation of water molecules about the *c*-axis using the adiabatic coincidence configuration (used in PIMD calculations).

$$H = -\frac{\hbar^2}{2I}\frac{\partial^2}{\partial\varphi^2} + \mathrm{V}(\varphi) \qquad \mathrm{V}(\varphi) = \frac{V_6}{2}(1 - \cos 6\varphi)$$

$$H_{nm} = \frac{\hbar^2 n^2}{2I}\delta_{n,m} + \frac{V_6}{4}\{2\delta_{n,m} - \delta_{n-m+6,0} - \delta_{n-m-6,0}\}, \quad n, m = 0, \pm 1, \pm 2, \ldots$$

m	E_m (meV) V_6=48 meV	ΔE (meV) V_6=48 meV	E_m (meV) V_6=56 meV	ΔE (meV) V_6=56 meV	ΔE (meV) average	Transitions (*m*=0)→(*m'*)
0	21.42		24.51			
1, 5	24.16	2.74	27.16	2.65	2.7	0→1, 0→5
2, 4	31.81	10.39	34.40	9.89	10.1	0→2, 0→4
3	38.73	17.31	40.51	16.0	16.7	0→3

The rotational energies E_m for water protons in beryl calculated by using six-fold potential with V_6=48 and 56 meV. The energies of the intraband ground state transitions ΔE, related to the tunneling peaks in INS spectra, and their assignments are shown.